1982

Laboratory Study of Trail-tube Irrigation

Mohamed O. Shanna

LABORATORY STUDY OF TRAIL-TUBE IRRIGATION

BY

MOHAMED O. SHANNA

A thesis submitted
in partial fulfillment of the requirement for the
degree Master of Science, Major in Engineering
South Dakota State University
1982

LABORATORY STUDY OF TRAIL-TUBE IRRIGATION

This thesis is approved as a creditable and independent investigation by a candidate for the degree, Master of Science, and is acceptable for meeting the thesis requirements for this degree. Acceptance of this thesis does not imply that the conclusions reached by the candidate are necessarily the conclusions of the major department.

Shu Tung Chu
Thesis Adviser
Date

Mylo A. Hellickson
Head, Agricultural Engineering Dept.
Date

ACKNOWLEDGEMENTS

The author wishes to express his appreciation to the People of the Socialist People's Libyan Arab Jamahiriya for the scholarship provided through the Secretariate of Dams and Water Resources. Without this scholarship I would not be able to continue my education.

Appreciation is extended to the entire Agricultural Engineering Department staff of South Dakota State University for their cooperation during this research. Dr. Dennis L. Moe, previous department head, is thanked for his welcoming me and for his assistance. Appreciation is also extended to Dr. Mylo A. Hellickson, Head of the Agricultural Engineering Department, for his cooperation, and to Dr. Darrell DeBoer for his help with the devices used in this research.

Special appreciation is extended to Dr. Shu T. Chu for his advice, guidance, and invaluable technical assistance throughout the course of the study.

MOS

TABLE OF CONTENTS

LIST OF FIGURES

LIST OF TABLES

PARTIAL LIST OF SYMBOLS

Symbol	Explanation	Units Used
A	Area	ft^2
a	Area	in^2
C	Hazen-Williams friction factor	- -
C_C	Coefficient of contraction	- -
cfs	Cubic feet per second	dfs (ft^3/sec)
C_Q	Coefficient of discharge	- -
C_V	Coefficient of velocity	- -
CV	Coefficient of variation	- -
D	Pipe diameter	ft, in
D_a	Depth of application	ft, in
d	Perforation diameter	in
dQ_x	Flow rate of an infitesmal line element, dx, on tube or flow rate of an infinitesmal perforation	gpm
F	Cumulative intake or the depth of infiltrated water	mm, in
f	Darcy-Weisbach's friction factor	- -
FF	F-factor of trail tubes after Christiansen (1942)	- -
g	Acceleration due to gravity = 32.16	ft/sec^2
gpm	Gallons per minute	gpm
H	Dimensionless total energy loss distribution or the distribution factor	- -
H_f	Head loss due to friction	ft
ID	Inside diameter	ft, in

PARTIAL LIST OF SYMBOLS CONTINUFD

Symbol	Explanation	Units Used
K_s	Scobey's friction factor	- -
L	Length of pipe or tube	ft
OD	Outside diameter	ft, in
P	Pressure head	Psi, ft, in
P_x	Pressure head at point x along the tube	Psi, ft, in
Psi	Pounds per square inch	lb/in^2
Q	Tube flow rate	gpm, cfs
Q_0	Total flow rate of a trail tube	gpm
q	Perforation flow rate	gpm, cfs
q_x	Perforation flow rate at a distance x along the tube	gpm
Q_x	Flow rate of trail tube at a distance x along the tube	gpm
R	Reynold's number	- -
R_H	Hydraulic radius = D/4 for round pipe flowing full	ft
S	Energy loss per foot of pipe = H_f/L	- -
SD	Standare deviation	- -
t	Time	min
TR	Time per revolution of a center pivot system	min
V	Average flow velocity	ft/sec
V_s	Traveling speed of a center pivot system	ft/min
ν	Kinematic viscosity	ft^2/sec

PARTIAL LIST OF SYMBOLS CONTINUED

Symbol	Explanation	Units Used
x	Distance from the first perforation at the upstream side of the tube to a point along the tube, where x is less than or equal L	ft
Z	Potential head or elevation	ft, in

INTRODUCTION

Increasing energy costs, continuing interest in more efficient use of water, and the availability of low cost plastic tubes initiated the idea of trail tube irrigation. Trail tubes are perforated poly-flex hoses similar to the laterals of a trickle irrigation system. These tubes connected to the main line of a center pivot system can be used to replace sprinklers. The main line of a center pivot system provides the water supply and the mobility. The arrangement of a trail tube irrigation system is similar to a traveling trickle system (Rawlins, et al., 1979).

Advantages of trail tube irrigation are its low energy consumption and its high water use efficiency. Trail tube operating pressures can be much lower than the pressure used in the conventional center pivot irrigation system. Such reduction in pressure represents a saving in energy consumption. Trail tubes also distribute water near the ground surface, which minimize water losses due to evaporation and wind effects. Decreasing water losses results in an improvement in water use efficiency.

A theoretical analysis of trail-tubes was presented in a paper, "Analysis of Irrigation by Trail Tubes", (Chu, 1982). The purpose of this study is to evaluate the theory by laboratory measurements.

The objectives of the study were:

1. To determine the roughness coefficient of the poly-flex hoses.
2. To determine the discharge coefficient of the perforations in the tubes.

3. To measure the average jet distance of the perforations.
4. To measure the distributions of flow rate and pressure along the tube.
5. To compare the measured distributions with the theoretical results.

LITERATURE REVIEW

Friction Loss Formulas

Water flow in pipes is accompanied by a loss of pressure due to friction. This loss depends on the roughness of the inside walls of the pipe, the diameter of the pipe, the viscosity of the water, and the velocity of the flowing water in the pipe. Many formulas for friction loss in pipes express the relationships between the factors involved. These empirical formulas have been developed from test data. The formulas most commonly used are:

A. Darcy-Weisbach's Formula (Pair, 1975)

$$H_f = f \frac{L}{D} \frac{V^2}{2g} \qquad (1)$$

Where H_f = the loss of pressure in pipeline, ft,

f = the friction factor,

L = the length of line, ft,

D = the pipe diameter, ft,

V = the average velocity, ft/sec, and

g = the acceleration due to gravity = 32.16 ft/sec^2.

In the above formula, the friction factor (f) depends primarily on the roughness of the pipe material, but also on velocity and pipe diameter. The friction factor values range from 0.015 for large smooth pipe to about 0.050 for very rough pipe, Christiansen (1942).

B. Hazen-Williams Formula (Brater and King, 1976)

$$V = 1.318\ C\ R_H^{.63}\ S^{.54} \qquad (2)$$

Where V = average velocity, ft/sec,

C = friction-loss coefficient,

R_H = D/4 for round pipe flowing full,

D is the diameter of pipe in ft, and

$S = H_f/L$ = energy loss per foot of pipe.

The typical values of the Hazen-Williams friction-loss coefficient (C), are given in Table 1.

Table 1: Hazen-Williams Friction Coefficient, C.

Type of Pipe	C Value
Extremely smooth and straight	140
Very smooth	130
New riveted steel	110
Old riveted steel	100
Old cast iron	95
Old pipes in poor condition	60 to 80

C. Scobey's Formula (Schwab, et al. 1966)

$$H_f = K_s \frac{L\, Q^{1.9}}{D^{4.9}} (1.45 \times 10^{-8}) \qquad (3)$$

Where H_f = total friction loss, ft,

K_s = Scobey's coefficient of retardation,

L = length of pipe, ft,

Q = total discharge, gpm, and

D = inside diameter, ft.

Valuis of K_s range from about 0.3 for smooth pipe to 1.0 or higher for very rough pipe (Christiansen, 1942).

It is confusing that f, C, and K_s have different names. However, they are similar in nature because they represent empirical constants in different friction formulas. To avoid confusion, these constants will be referred to as friction coefficients in the following study.

Flow Formula and Orifice Coefficient

The flow rate in pipes and orifices can be described by the continuity equation and the orifice flow formula.

Pipe Flow: Based on the conservation of mass principle, the flow rate of water in a pipe is represented by the product of average velocity of the water and cross-sectional area of the pipe (Pair, et al. 1975).

$$Q = A\,V \tag{4}$$

Where Q = flow rate, cfs,

A = cross-sectional area of flow, ft^2, and

V = average velocity of flow, ft/sec.

Orifice Flow: An orifice is an opening with closed circumference through which water flows (Brater and King, 1976). The flow rate of an orifice is described by the orifice flow equation

$$Q = A\,C_Q(2gh)^{0.5} \tag{5}$$

Where Q = discharge, cfs,

A = cross-sectional area of the orifice, ft^2

C_Q = the coefficient of discharge which is the product of the coefficient of contraction (C_C) and the coefficient of velocity (C_V),

g = acceleration of gravity, ft/sec, and

h = the pressure head, ft

For practical convenience the orifice flow equation can be written in the following way (Christiansen and Davis, 1967).

$$q = 38\ C_Q\ a\ (P)^{0.5} \qquad (6)$$

Where q = discharge, gpm,

a = orifice area, in^2,

P = pressure head as presented in psi.

The discharge coefficient of an orifice has been the topic of many studies. Hamilton Smith, 1886 (in Brater and King, 1976), reported that for circular orifices with a diameter of 0.02 feet, the discharge coefficients (C_Q) were found to be 0.632 and 0.611 at a pressure head of 2 and 10 feet, respectively. The C_Q was 0.595 for a diameter of 1 foot at heads of 2 and 10 feet.

Values of the discharge coefficient for 1 inch orifices were determined by various investigations and were found to be different. The differences are not entirely due to experimental error. Other factors may contribute, for example the ratio of the orifice diameter to the tank wall, the sharpness of the orifice edge, the smoothness of the inner surface, the orifice plate, and the temperature of the water. When the tank wall thickness is close to the size of the orifice diameter, the contraction will be suppressed and C_Q approaches the value of C_V (Brater and King, 1976).

The relation between Reynold's number (R) and C_Q was presented by Brater and King (Figure 12). The dotted line (A-B) in this Figure was the range of R covered by the tests of Medaugh and Johnson (1940). In this range, the C_Q was approximately a constant, equal to 0.60.

A discharge coefficient of 0.6 for a sharp-edged orifice, a standard orifice, can be found in many text books, for example Pederson (1971).

Trail-Tube Irrigation

The development of economical plastic tubes during the 1950's helped initiate the practice of trickle irrigation. Such a system applies water at a low rate through mechanical devices, called emitters, located at selected points along plastic tubes. In the 1970's, the research in trickle irrigation entered its well developed stage. The two major problems associated with this type of irrigation were the clogging of the emitters and the high cost of the total quantity of material (Howell, et al., 1980). These problems prompted the introduction of traveling trickle systems. On a trail tube, many small orifices can be substituted by a small number of large orifices to diminish the hazard of clogging. Furthermore, a traveling tube can replace many stationary tubes to reduce the total material cost (Rawlins, et al. 1979).

The traveling trickle system did not receive widespread acceptance because there was no adequate carrier to provide mobility. A traveling sprinkler system was suggested to be used as a carrier for the trickle tubes (Rawlins, et al., 1979), but the replacement of sprinklers with traveling tubes on a center pivot system did not seem to be attractive at that time.

Increasing energy costs and the desire for increased water-use efficiency gradually shifted research interest toward trail tube irrigation. Since 1978, extensive research on trail-tube systems has been conducted in the states of California, Texas, Arizona, and Idaho (Howell, Phene, and Sanders, 1980). These studies utilized the mainframe of a linear-travel sprinkler system as a carrier and water source for trail tubes. A practical difficulty associated with using a linear-travel sprinkler system as a carrier is that the direction of trail tubes has to be reversed at the end of the field so that irrigation can be continued on its returning trip. In this study, the frame of a center pivot irrigation system is to be used as a carrier for the trail tubes. The traveling path of a center pivot system is in concentric circles, and the direction of travel normally does not reverse during operations. The existing difficulty of a linear carrier is avoided by a center pivot tube carrier.

A trail tube is a specific type of irrigation lateral because of its unique application pattern. The fluid mechanics of an irrigation lateral consist of two parts: the total friction loss, and the dimensionless pressure distribution of an irrigation lateral (Chu, 1982).

The friction loss of a lateral in a hand move irrigation system was studied by Christiansen (1942). He introduced an F factor to represent the friction loss of a lateral as a fraction of the friction loss of an associated supply pipe which has the same characteristics. These characteristics include size, length, surface roughness, and total flow rate similar to those of a lateral (Christiansen, 1942). Merrian (1968) described the pressure distribution of a lateral in a hand move irrigation system. He mentioned that a little over 50% of the pressure loss occurs in the first 1/5 of the length, and about 87% in the first 1/2. Chu and Moe (1972) investigated the fluid mechanics of a center pivot irrigation system. They obtained the F factor of a center pivot irrigation system and introduced a distribution factor to describe the pressure distribution of a center pivot system. Chu (1982) defined the distribution factor as a normalized version of the energy grade line. The energy grade line as defined by Brater and King (1976) is the line representing the total energy at any point. Wu, Howell, and Hiler (1979) studied the hydraulics of the lateral in a trickle irrigation system in detail. They prepared design charts for trickle laterals under various operating conditions including conditions of non-uniform slopes and conditions of varying pipe sizes.

Soil Intake Families

The water intake by soils, Soil Conservation Service (SCS, 1964) is the movement of irrigation water from the surface into and through the soil. Water intake is the expression of several factors including infiltration and percolation.

The classification of soils into intake families or groups is based upon analyzing cylinder-infiltrometer data from large numbers of sites. Soil of minor differences are considered together as a group. The SCS (1976) classified soils into eight intake families or groups. These groups have been assigned numbers such as 0.1, 0.3, . . . 4.0. These numbers approximate the basic-rate values for soils in those families. The basic intake rate is the nearly constant rate developed after some time has elapsed from the start of irrigation. The time required to infiltrate a certain depth of water cah be calculated by using the equation of the intake families used by SCS, (Hart, 1980). This equation can be written as follows:

$$F = a\ t^{b} + c$$

Where F = the cumulative intake or the depth of infiltrated water, mm,

t = the time required to infiltrate a certain depth of water, min, and

a, b, and c = constants associated to each intake family.

Values of the constants are shown in Table 2.

Table 2: Constants for Different Intake Families. (Adapted from ASAE, Monograph No. 3, 1980.

Intake family	a	b	c
0.05	0.5334	0.618	7.0
0.10	0.6198	0.661	7.0
0.15	0.7110	0.683	7.0
0.20	0.7772	0.699	7.0
0.25	0.8534	0.711	7.0
0.30	0.9246	0.720	7.0
0.35	0.9957	0.729	7.0
0.40	1.0640	0.736	7.0
0.45	1.1300	0.742	7.0
0.50	1.1960	0.748	7.0
0.60	1.3210	0.757	7.0
0.70	1.4430	0.766	7.0
0.80	1.5600	0.773	7.0
0.90	1.6740	0.779	7.0
1.00	1.7860	0.785	7.0
1.50	2.2840	0.799	7.0
2.00	2.7530	0.808	7.0

Methods and Procedures

Theory

The theory of trail-tube hydraulics (Chu, 1982) can be divided into three parts: tube flow rate distribution, total friction loss, and pressure distribution.

The tube flow rate is described by the following equation.

$$\frac{Q_x}{Q_0} = 1 - B\left(\frac{x}{L}\right)^{0.5} - (1 - B)\frac{x}{L} \qquad (8)$$

Where Q_0 = total flow rate of trail tube,

Q_x = the flow rate at a distance x from the upstream end of the tube,

L = the length of the trail tube,

$B = A_0(VL)^{0.5}/[A_0(VL)^{0.5} + A_1L]$ = a constant,

V = the constant traveling speed of the trail tube, and

A_0 and A_1 are the infiltration parameters of Philip's model (1957).

The total friction loss is given by the following equation.

$$\frac{H_0}{H_f} = F = \int_1^0 \left[1 - B\left(\frac{x}{L}\right)^{0.5} - (1 - B)\frac{x}{L}\right]^{1.85} d\left(\frac{x}{L}\right) \qquad (9)$$

Where H_0 = the total friction loss of a perforated tube,

H_f = the total friction loss of the trail tube without perforations, and

F = the F factor of trail tube.

The pressure distribution is represented by the following equation.

$$H = \frac{H_x}{H_0} = \frac{1}{F} \int_{1}^{x/L} [1 - B\ (\frac{x}{L})^{0.5} - (1 - B)\ \frac{x}{L}]^{1.85}\ d(\frac{x}{L}) \quad (10)$$

Where H = the distribution factor of the trail tube after Chu (1982), and

H_x = the friction loss from the point x to the downstream end of tube.

A graphical representation of equations 8, 9, and 10 is provided in Figures 1, 2, and 3, respectively, to facilitate their application in practice. These Figures are the same as the Figures provided by Chu (1982). The numerical procedure to obtain these curves is provided in Appendix C.

The theory was based upon the assumptions that the energy associated with the flow velocity, the kinetic energy, is usually small, and can be geglected, and that the land is level. It was observed in this study that the kinetic energy in the trail tubes was substantial, which contradicts the assumptions made in the previous study (Chu, 1982). However, based upon conservation of energy principle, the theory can be extended to the condition where the land has uniform slopes and where the kinetic energy is not neglible by modifying equation 10. This modified equation represents the distribution of total energy loss rather than the pressure distribution. The modified version of the trail tube theory is to be evaluated in this study.

In the derivation of theoretical results, Equations 8 to 10, the perforation flow rate was represented by the orifice flow formula

$$Q_2 - Q_1 = dQ_x = 38\ C_Q\ a\ (P_x)^{0.5}$$

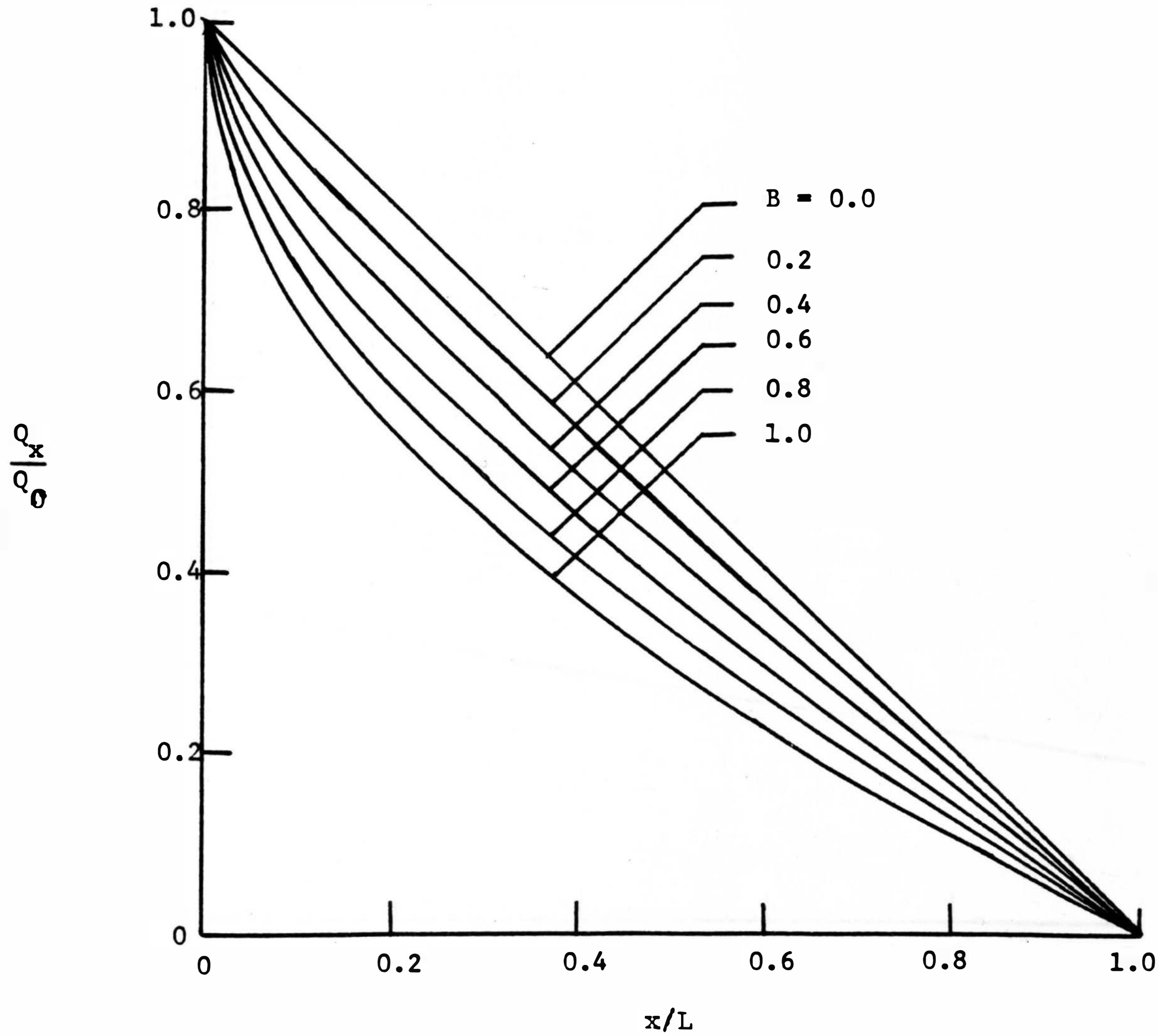

Figure 1: Dimensionless Tube Flow Rate Distribution; Symbols Defined in Equation 8.

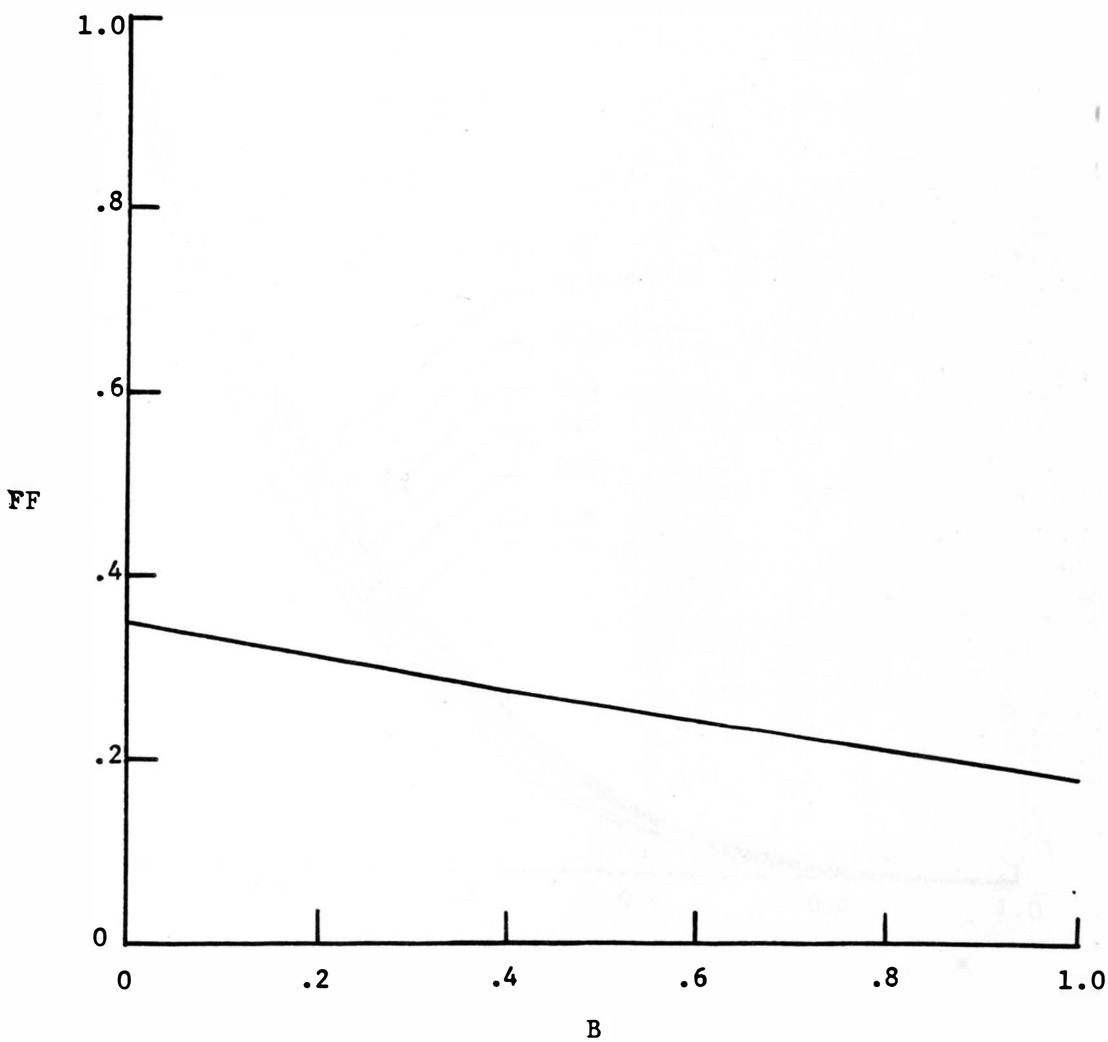

Figure 2: F factor of Trail Tubes; Symbols Defined in Equations 10 and 8.

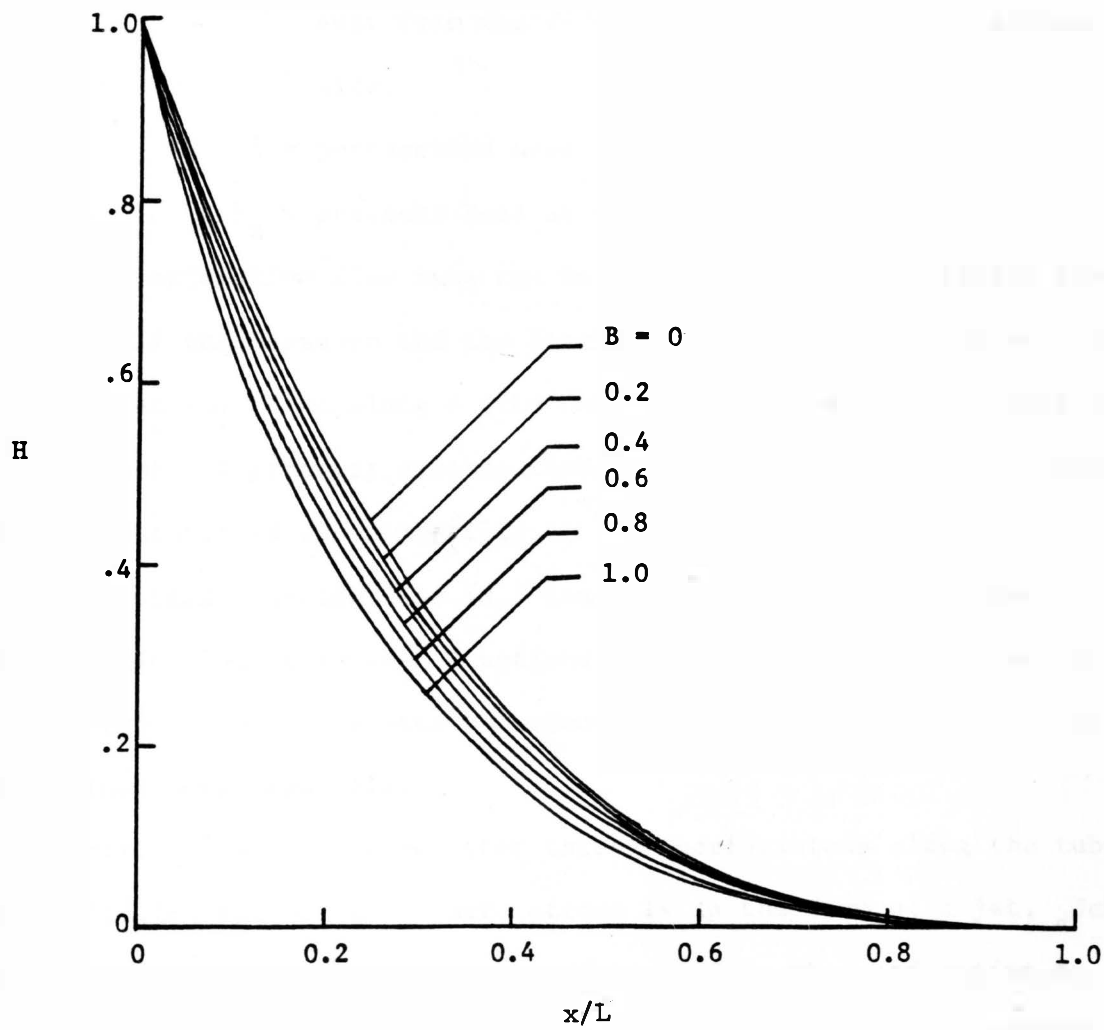

Figure 3: Dimensionless Total Energy Loss Distribution (H) of Trail Tubes; Symbols Defined in Equations 8 and 10.

Where Q_2 = the tube flow rate upstream of a perforation,

Q_1 = the tube flow rate downstream of a perforation,

dQ_x = the change of the tube flow rate at a distance x away from the first perforation at the upstream side,

a = perforation area in square inches, and

P_x = pressure head at point x.

The perforation flow rate can be obtained using the orifice flow formula, if the pressure and the discharge coefficient are given. The pressure at any point along a tube can be determined with the help of the theoretical pressure distribution, but the discharge coefficient must be determined experimentally.

The total friction loss (H_f) can be calculated by using one of the friction loss formulas, Equations 1, 2, and 3. But the friction coefficient which represents the smoothness of tube material must be determined experimentally.

Trail-tubes distribute water through perforations along the tubes. Water flowing out of these perforations is in the form of a jet. Jet distance is the maximum horizontal distance from the perforation to the jet fall, Figure 7. This distance is controlled by the operating pressure. A relationship between the pressure and the jet distance is needed in practice to select an appropriate tube spacing. Jet distance will be investigated by laboratory measurements in this study.

Friction Coefficient Determination

Friction loss was measured by the difference of water level in two manometers established at both ends of a poly-flex hose, Figure 5. Two pressure regulators connected in series were used to maintain constant pressure during measurement, Figure 4. The tube flow rate was controlled by a gate valve and was measured by using a water-meter and a stop watch. A pressure differential range from 1 to 10 feet of water was used in the tests. Three tube sizes, including tube diameters of 1/2, 3/4, and 1 inch, were investigated. Tube length was 25 feet for testing the 1/2 inch tube and was 50 feet for other sizes.

The measured friction loss under different flow rates was analyzed to evaluate the friction coefficient in a pipe friction model. Three models were evaluated in this study, including the Darcy-Weisbach formula, the Hazen-Williams formula, and Scoby's formula, Equations 1, 2, and 3. The model which provided the least variation in thr friction coefficient was to be selected to test the theoretical results.

Discharge Coefficient Determination

Ten equally spaced holes were drilled in a five foot tube. A manometer was established at each end of the tube, Figure 6. This tube was connected to a water-meter, two pressure regulators, and a flow control valve at the water source, Figure 4. Pressure regulators were used for controlling the pressure at the upstream side of the tube. The pressure was measured by the height of the water in the manometer. Average values of the pressure readings from the two manometers were used to represent the operating pressure.

Flow rates were measured from each of the ten perforations by a graduated cylinder and a stop watch. The value of each perforation

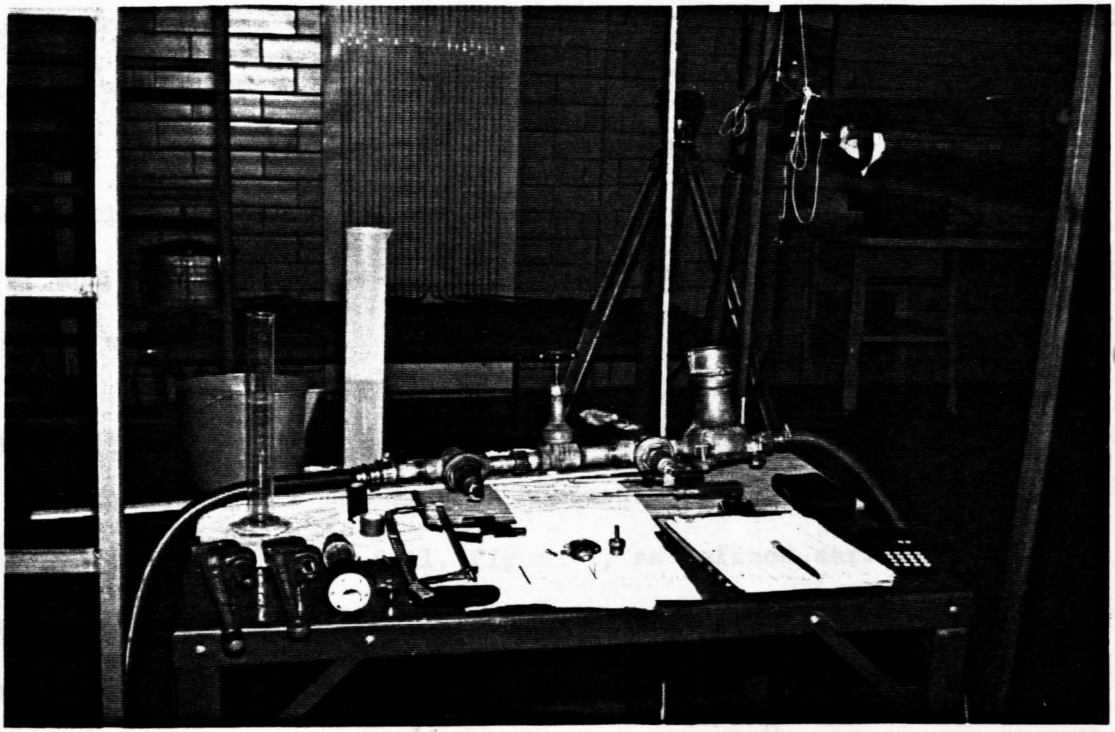

Figure 4: Pressure Regulations, Flow Control Value, Water Meter, and Surveying Instrument.

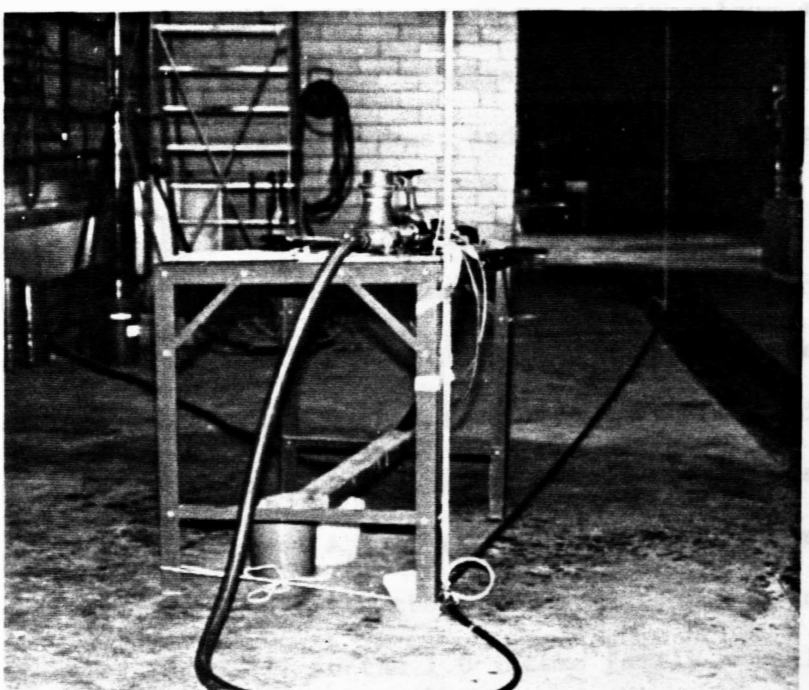

Figure 5: Poly-Flex Tube and Manometers for Friction Loss Measurements.

flow rate was used to determine the discharge coefficient in the orifice flow formula, Equation 6.

The discharge coefficients were obtained for three sizes of perforations 1/16, 5/64, and 1/8 inch with three sizes of tubes 1/2, 3/4, and 1 inch in diameter under a pressure head ranging from 2 to 10 feet of water.

Jet Distance

Jet distance is the maximum horizontal distance from the perforations to the jet fall, Figure 7, as defined earlier. Jet distance was measured after determining the discharge coefficient, using the same perforated tubes, in the following manner: The perforated tubes were oriented at an angle of 45^o with respect to the ground surface. Under such an angle the jet distance reaches its maximum. Average maximum jet distances of ten perforations were measured in this study. These measurements were determined for each tube size, for three perforation sizes, and at five pressures.

Distribution of Tube Flow Rate and Pressure

The distribution of tube flow rate determines the application pattern of a trail tube. Philip's infiltration model was used for matching the application pattern of trail tubes to the soil infiltration characteristics (Chu, 1982). There were two parameters included in this model, A_0 and A_1, Equation 8. A following numerical example is presented to illustrate the procedures to determine these parameters for a typical soil in the 1.0 intake family. Philip's

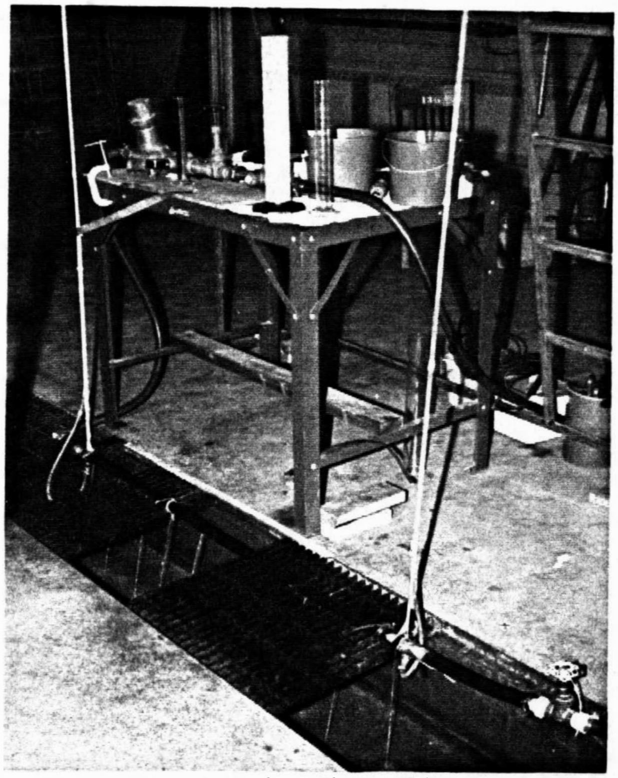

Figure 6: Perforated Poly-Flex Tube and Manometers For Flow Rate Measurement

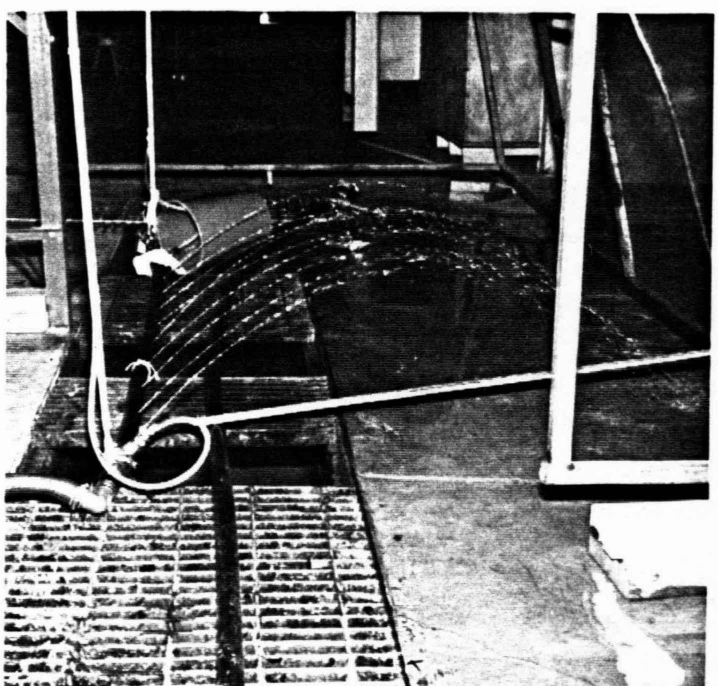

Figure 7: Perforated Poly-Flex Tube for Jet Distance Measurement

infiltration model (1957) is represented by

$$F = A_0\ t^{0.5} + A_1\ t \tag{11}$$

Where F = the cumulative infiltration, in, and

t = the infiltration time, min.

From Table 2, the constants for the 1.0 intake family are, a = 1.786, b = 0.785, and c = 7. Substituting these constants in equation (7) results in

$$F = 1.786\ t^{0.785} + 7$$

Rearrangement of this equation gives

$$t = \left(\frac{F - 7}{1.786}\right)^{1.2739} \tag{12}$$

Where F = the accumulative intake or the depth of infiltrated water, mm.

Substituting in equation (12) for

F = 1 inch (25.4 mm), t = 19.5 minutes (13)

and for F = 2 inch (50.8 mm), t = 58.9 minutes.

Substituting in equation number (11)

for F = 1, and t = 19.5, results in

$$1 = A_0\ (19.5)^{0.5} + (19.5)\ A_1 \tag{14}$$

for F = 2, and t = 58.9, results in

$$2 = A_0\ (58.9)^{0.5} + (58.9)\ A_1 \tag{15}$$

By solving equation (14) and (15) results in

A_1 = 0.0009 ft/min (0.0105 in/min), and

(16)

A_0 = 0.0150 ft/min$^{0.5}$ (0.1801 in/min$^{0.5}$)

Perforation size has a direct effect on the tube flow rate. Selection of perforation size depends on two factors: Hole size and clogging. Small holes are desirable because more holes along the tube provide more precision for tube flow adjustments. However, too small a hole should not be used because of clogging.

The United States Department of Agriculture classifies soils into different groups according to texture (Schwab, et al., 1966). These groups are gravel, sand, silt, and clay. The particle size range of these groups are: more than 2, 2 to 0.05, 0.05 to 0.002, and less than 0.002mm, respectively. For this study, the smallest recommended perforation size that will allow the passage of large particles (sand 2 mm) is 5/64 inch (2 mm).

The theoretical distribution of tube flow rate and pressure were tested for the conditions of the outermost trail tube on a center pivot system. The radial distance from this tube to the pivot is 1317.5 feet, Figure 9. The center pivot system is designed to apply one inch of water (depth of application) in a period of 3 days (time per revolution). The system is assumed to irrigate on a 1.0 intake family soil, Table 2. The infiltration parameters of 1.0 intake family soil are A_0 = 0.015 ft/min$^{0.5}$, A_1 = 0.0009 ft/min (Equation 16) and the time required to infiltrate 1.0 inch of water was 19.5 minutes, Equation 13.

The following procedure is used to determine the length of tube. Let V_s be the traveling speed of the center pivot system at a distance equal to r from the pivot, Figure 9. Therefore,

$$V_s = \left(\frac{2\pi r}{TR}\right) \tag{17}$$

Where V_s = system traveling speed, ft/min,

$2\pi r$ = the circumference of a circle with a radius r, ft, and

TR = the time per revolution of a center pivot system, min.

The center pivot system is designed to travel a distance equivalent to the tube length, L, within a period of time, t, which is the time of application described in equation 12. So

$$V_s = \frac{L}{t} \tag{18}$$

Where L = tube length, ft, and

t = the time required to infiltrate a depth of water needs to be applied, min.

Combine equations 17 and 18 to obtain

$$L = (\frac{2\pi r}{TR})\ t \tag{19}$$

$$L = (\frac{2\pi\ (1317.5)}{3 \times 24 \times 60})\ 19.5 = (1.9162)\ 19.5 = 37.4 \text{ feet}$$

The tube discharge (Q_0) can be calculated as follows. Let the area to be irrigated by the tube equal A, and the depth of the application equal D_a. Therefore, the volume of water to be applied equals the product of A and D_a. This volume to be applied in a time equal to TR. So the tube flow rate is

$$Q_0 = (\frac{A(D_a)}{TR})\ 7.48 \tag{20}$$

Where A = tube irrigated area, ft^2

D_a = depth of application, ft.

7.48 = conversion factor.

Tube spacing is selected to be 5 feet in this study. This spacing is equivalent to having one tube in every other crop row. The irrigated area covered by the tube is

$$A = \pi(r^2 - r_1^2), \text{ Figure 9}$$

Where r = radial distance from the pivot center, ft, and

$r_1 = r - 5$ feet

$$A = \pi[(1320)^2 - (1315)^2] = 41390.5 \text{ ft}^2$$

D_a = 1 inch = 1/2 ft (0.0833 ft)

TR = (3)(24)(60) = 4320 min

$$Q_0 = \left(\frac{41,390.48\ (0.0833)}{4320}\right) 7.48 = 5.97 \text{ GPM}$$

The B - value for use in equation 8 was calculated

$$B = [A_0(VL)^{0.5}]/[A_0(VL)^{0.5} + A_1 L]$$

$$B = [0.015(1.92 \times 28)^{0.5}]/[0.015(1.92 \times 38)^{0.5} + 0.0009(38)]$$

$$B = 0.79$$

Perforation spacing was calculated starting from the downstream end and working upstream. Minimum operating pressure of 2 pounds per square inch (psi) was selected for the downstream end of the tube, Table 6. The calculations follow the procedure described by Chu (1982). A numerical example is shown below for a tube 3/4 inches in diameter.

Tube cross-sectional area (A) $= \frac{\pi D^2}{4} = \frac{\pi(0.0628)^2}{4} = 0.0031 \text{ ft}^2$

$Q_0 = (5.79)(0.002228) = 0.129$ cfs

Hydraulic radius of tube (R_H) $= \frac{D}{4} = \frac{0.0628}{4} = 0.0157$ ft.

Substituting H_f/L for S and solving for H_f equation 2 becomes:

$$H_f = \left[\frac{V}{1.318\ C\ (\frac{D}{4})^{0.63}}\right]^{1.85} (L), \text{ thus} \qquad 2A$$

$$H_f = \left[\frac{4.1613}{1.318(135)(0.0157)^{0.63}}\right]^{1.85} (38)$$

$$H_f = 4.62 \text{ ft}$$

From Figure 2, F = 0.214 for B = 0.79.

From equation (9), the total friction loss of the perforated tube

$$H_0 = (F)(H_f) = (0.214)(4.62) = 0.99 \text{ ft}$$

From Figure 3, H = 0.0 for x/L = 1.0 (tube end)

From equation (10)

$$H_x = (H)(H_0) = (0.0)(0.99) = 0.0 \text{ ft of water}$$

The pressure at the tube end

$$P_x = H_x + P_1$$

$$= 0.0 + 4.62 = 4.62 \text{ ft of water (2 Psi)}$$

From the orifice flow formula, Equation (6)

$$q = 38\ C_Q\ a\ (P_x)^{0.5}$$

For the perforation diameter (d) = 5/64 inch,

area (a) = $(\pi\ d^2)/4 = \frac{\pi(0.0781)^2}{4} = 0.0048\ \text{in}^2$,

$$q = 38(0.65)\ (0.0048)(P_x)^{0.5}, \quad (C_Q = 0.65 \text{ from Table 5})$$

$$q = 0.1184\ (P_x)^{0.5} \qquad (21)$$

The flow rate from the first perforation on the downstream side is determined using equation (21).

$$q = 0.1184(2)^{0.5} = 0.1674 \text{ gpm}$$

From Figure 1, $Q_x/Q_0 = 0.0$ for B = 0.79 and x/L = 1.0

$$Q_x = (Q_0)(0.0) = 0.0, \text{ where } Q_x = \text{tube discharge just beyond } q_1.$$

The tube flow rate at the next perforation upstream (Between perforation 1 and 2), is

$$Q = Q_x + q_x = 0.0 + 0.1674 = 0.1674 \text{ gpm, and}$$

$$Q/Q_0 = \frac{0.1674}{5.79} = 0.0289$$

From Figure 1, the values of x/L are

$$x/L = 1 \text{ when } Q_x/Q_0 = 0.0$$

$$x/L = 0.95 \text{ when } Q/Q_0 = 0.0289$$

Therefore, the spacing between the adjacent perforations (1 and 2) is

$$(1 - 0.95)L = 0.05(38) = 1.9 \text{ ft}$$

From Figure 3, for B = 0.79 (Equation 8)

$$H = 0.0 \text{ for } x/L = 0.95$$

From equation (10)

$$H_x = 0.0(0.99) = 0.0 \text{ ft of water}$$

The pressure at $x/L = 0.95 = P_x$

$$P_x = H_x + P_1 = 0.0 + 4.62 \text{ ft of water (2 Psi)}$$

From equation (21)

$$q = 0.1184(2)^{0.5} = 0.1674 \text{ gpm}$$

Tube flow rate at the next perforation upstream (between perforation 2 and 3) is

$$Q = Q_x + q_x = 0.01674 + 0.1674 = 0.3348 \text{ gpm}$$

$$Q/Q_0 = \frac{0.3348}{5.79} = 0.0578$$

From Figure 1, the values of x/L are

$$x/L = 0.95, \text{ when } Q_x/Q_0 = 0.0289$$

$$x/L = 0.905, \text{ when } Q/Q_0 = 0.0578$$

So, the spacing between perforation 2 and 3 equals

$$(0.95 - 0.905)38 = 1.71 \text{ ft}$$

The procedures were continued until the discharge and the tube length were close to 5.79 gpm and 38 feet, Table 3.

Based upon the information calculated in Table 3, thirty-four 5/64 inch perforations were drilled in a 3/4 inch poly-flex tube. Six manometer tubes were installed at 0.0, 3.8, 11.4, 19.0, 28.5, and 38.0 feet to obtain the distribution of total energy loss, Figure 8. Pressure regulators were used for controlling the pressure required at the upstream side of the tube. The elevations along the tube at the six manometers taps were measured by using a surveying level. A gate valve and two pressure regulators were used to control water flow.

Flow rate through each perforation was determined by a graduated cylinder and a stop watch. Perforation flow rates were accumulated to obtain the tube flow rate distribution.

Figure 8: Perforated Poly-Flex and Six Manometers to Measure the Flow Rate and Pressure Distribution

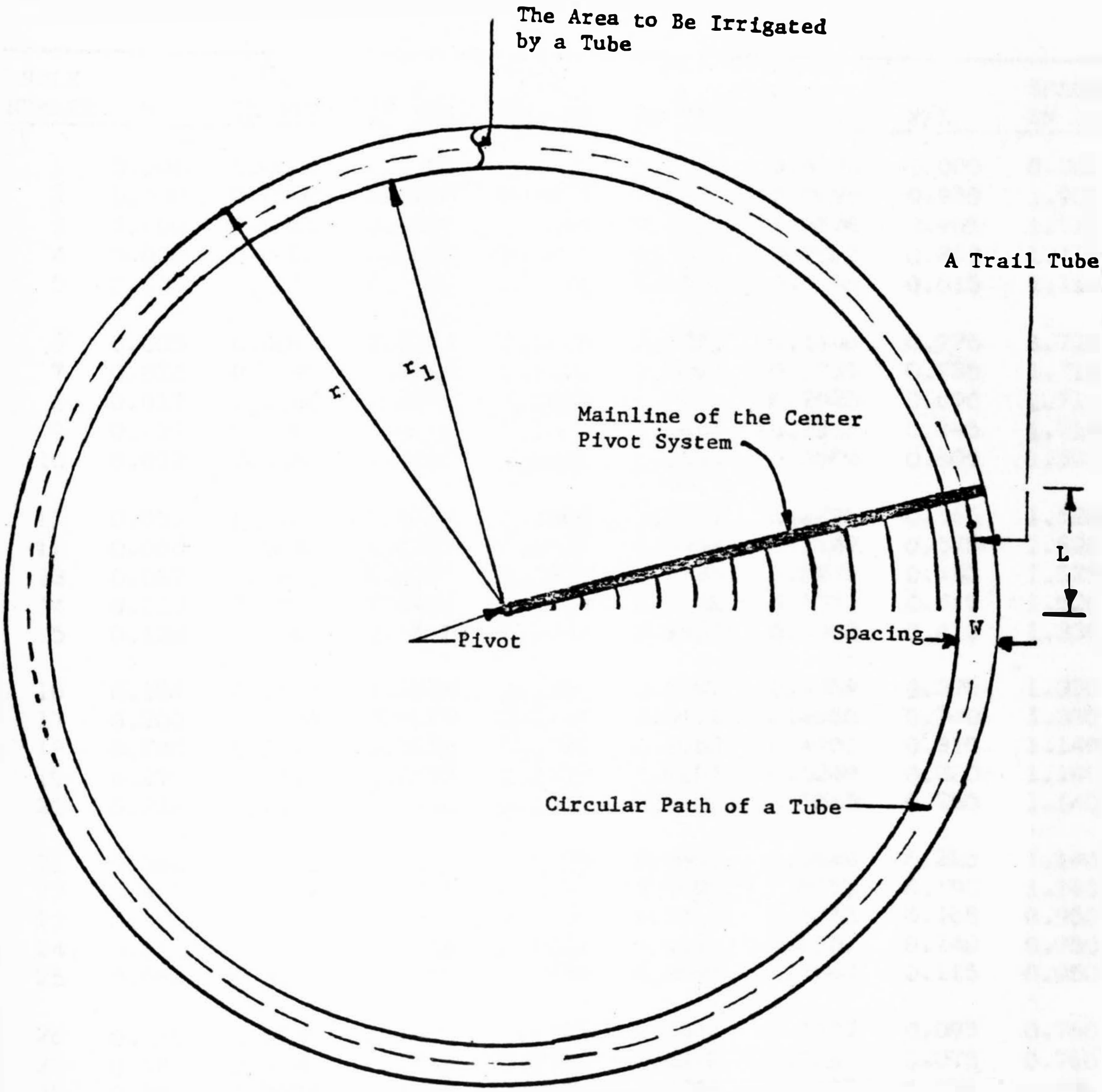

Figure 9: Schematic Diagram of Trail-Tube and Center Pivot System Showing the Area to be Irrigated by the Outer Tube, and the Symbols Used For Calculation.

Table 3. Perforation Spacing Along the Trail Tube

HOLE NUMBER	H	H_x IN FEET	P_x IN PSI	q_x IN GPM	Q_x IN GPM	Q_x/Q_0	x/L	SPACING IN FEET
1	0.000	0.0000	2.0000	0.1674	0.0000	0.0000	1.000	0.000
2	0.000	0.0000	2.0000	0.1674	0.1674	0.0289	0.950	1.900
3	0.000	0.0000	2.0000	0.1674	0.3348	0.0578	0.905	1.710
4	0.000	0.0000	2.0000	0.1674	0.5022	0.0867	0.860	1.710
5	0.000	0.0000	2.0000	0.1674	0.6692	0.1156	0.815	1.710
6	0.005	0.0049	2.0021	0.1675	0.8371	0.1446	0.775	1.710
7	0.010	0.0099	2.0043	0.1676	1.0047	0.1735	0.735	1.710
8	0.017	0.0168	2.0073	0.1677	1.724	0.2025	0.690	1.710
9	0.027	0.0267	2.0116	0.1679	1.3403	0.2315	0.645	1.710
10	0.039	0.0386	2.0167	0.1681	1.5084	0.2605	0.605	1.520
11	0.050	0.0495	2.0214	0.1683	1.6767	0.2896	0.565	1.520
12	0.068	0.0673	2.0291	0.1687	1.8454	0.3187	0.525	1.520
13	0.088	0.0871	2.0377	0.1690	2.0144	0.3479	0.485	1.520
14	0.110	0.1089	2.0471	0.1694	2.1838	0.3772	0.445	1.520
15	0.138	0.1366	2.0591	0.1699	2.3537	0.4063	0.410	1.330
16	0.169	0.1673	2.0724	0.1704	2.5241	0.4359	0.375	1.330
17	0.200	0.1979	2.0857	0.1710	2.6951	0.4655	0.340	1.330
18	0.240	0.2375	2.1028	0.1717	2.8668	0.4951	0.310	1.140
19	0.275	0.2722	2.1178	0.1723	3.0391	0.5249	0.280	1.140
20	0.316	0.3127	2.1354	0.1730	3.2121	0.5548	0.250	1.140
21	0.364	0.3603	2.1560	0.1738	3.3859	0.5848	0.220	1.140
22	0.412	0.4078	2.1765	0.1747	3.5606	0.6150	0.190	1.140
23	0.462	0.4572	2.1979	0.1755	3.7361	0.6453	0.165	0.950
24	0.510	0.5047	2.2185	0.1764	3.9125	0.6757	0.140	0.950
25	0.564	0.5582	2.2416	0.1773	4.0898	0.7064	0.115	0.950
26	0.625	0.6186	2.2678	0.1783	4.2681	0.7372	0.095	0.760
27	0.680	0.6730	2.2913	0.1792	4.4473	0.7681	0.075	0.760
28	0.735	0.7274	2.3149	0.1801	4.6274	0.7992	0.055	0.760
29	0.800	0.7918	2.3428	0.1812	4.8086	0.8305	0.042	0.475
30	0.840	0.8313	2.3599	0.1819	4.9905	0.8619	0.030	0.475
31	0.885	0.8759	2.3792	0.1826	5.1731	0.8935	0.022	0.304
32	0.920	0.9105	2.3942	0.1832	5.3563	0.9251	0.015	0.266
33	0.940	0.9303	2.4027	0.1835	5.5398	0.9568	0.008	0.266
34	0.968	0.9580	2.4147	0.1840	5.7238	0.9886	0.001	0.266

Results and Discussion

Friction Coefficient

The measured friction losses for different flow rates of the poly-flex tubes are listed in Table A (Appendix A). The measured friction loss (H_f) as influenced by the velocity for three poly-flex tube sizes is plotted in Figure 10 for practical application. The following three pipe friction formulas were used to obtain the friction coefficients: Darcy-Weisbach's formula, Hazen Williams formula, and Scobey's formula. Variation in friction coefficient was evident for different sizes of tubes, Table 4.

A coefficient of variation (CV) was calculated for each pipe friction model to represent the variation of friction coefficient. Hazen-Williams friction coefficient (C) gives the lease CV, Table 4; 2 percent as compared with 12 percent for the Darcy-Weisbach and 16 percent for the Scobey. Thus, Hazen Williams formula was selected to represent the friction loss of poly-flex hoses.

The average friction coefficient (C) values were 135 for 3/4 inch (ID = 0.7536) and 1 inch (ID = 1.0363), and 130 for 0.5 inch (ID = 0.552) tubes, Table 4.

To investigate the type of flow in the trail tube, the Darcy-Weisbach friction coefficient (f), and Reynold's number are plotted on Moody's diagram, Figure 11. Almost all the measured data points fall in the transition zone and close to the smooth pipe region. This result shows that poly-flex tubes were hydraulically smooth pipes and the type of flow was generally turbulent.

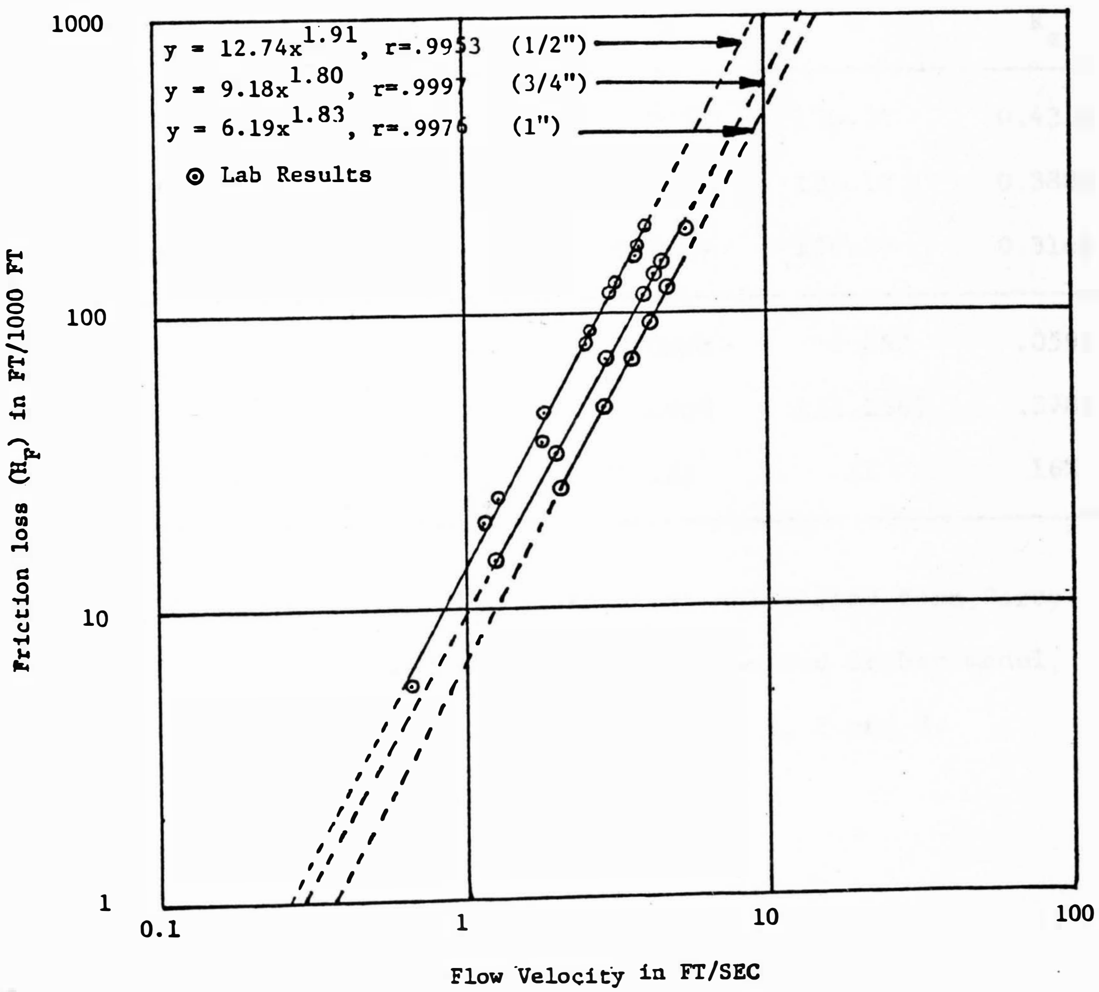

Figure 10: Relation Between Friction Loss in ft Per 1000 ft of Pipe, and the Flow Velocity in ft/sec.

Table 4. Friction Coefficient of Poly-Flex Tubes

Tube size in inches		Friction Coefficients		
OD	ID	f	C	K_s
0.50	0.552	0.0352	130.35	0.4330
0.75	0.7536	0.0294	135.13	0.3888
1.00	1.0363	0.0279	134.29	0.3144
SD		0.0038	2.552	.0599
$\overline{X}$		0.0308	133.2567	.3787
CV		12%	2%	16%

Where f, C, and K_s - friction coefficient calculated from Darcy-Weisbach, Hazen-Williams and Scobey model, respectively, Equations 1, 2 and 3.

SD - standare deviation

$\overline{X}$ - the mean value

OD - outside diameter

ID - inside diameter

CV - coefficient of variation

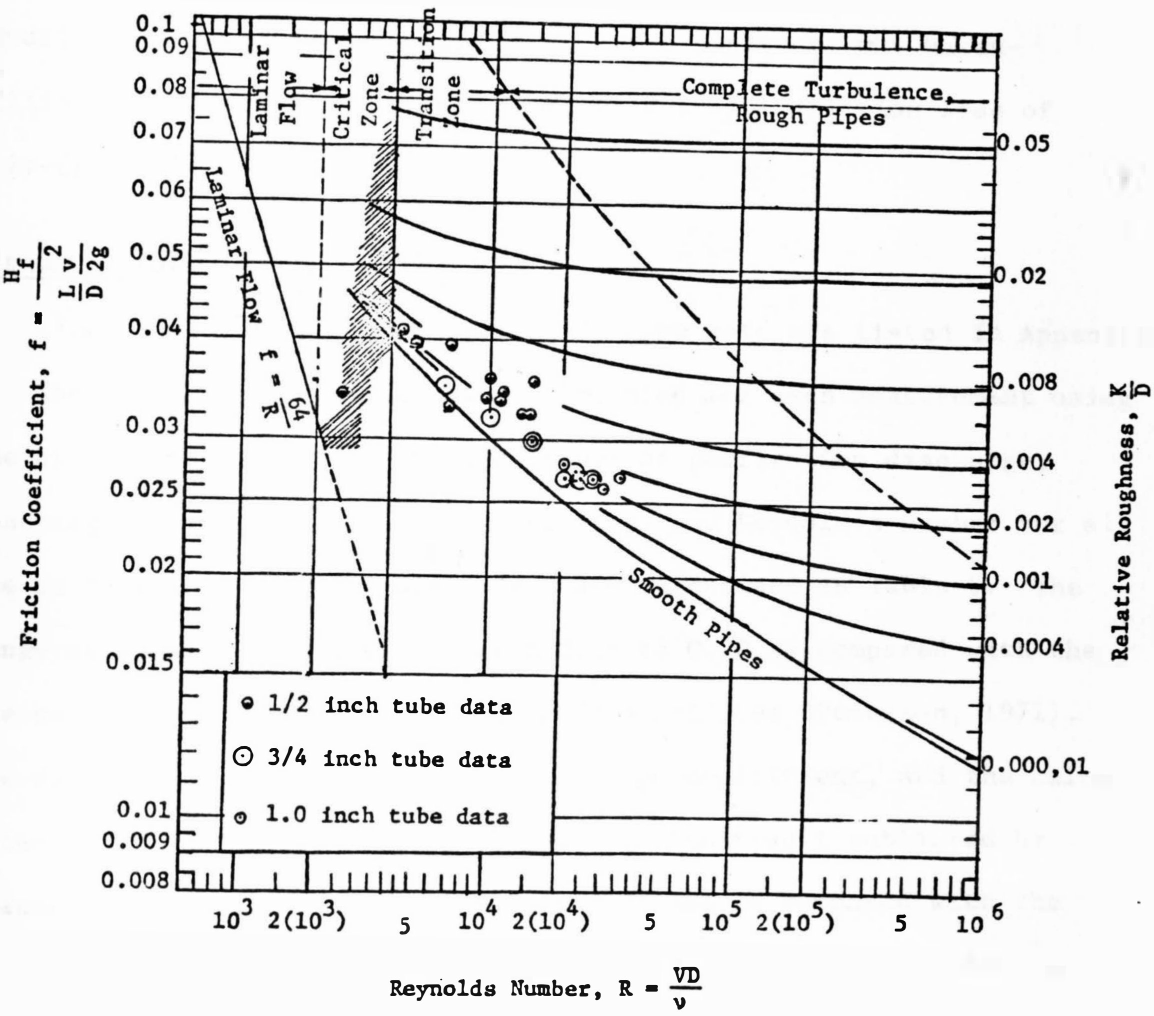

Figure 11: Measured Darcy-Weisbach Friction Coefficient on Moody's Diagram. (Adapted from, Trans. ASME, 1944).

For smooth pipes the friction loss for turbulent flow depends on flow velocity. Vennard (1961) reported that friction loss is proportional to $V^{1.75}$. It will be noted on page 25 that H_f in the equation 2A is proportional to $V^{1.85}$. This explained why Hazen-Williams formula was a suitable model to describe friction loss of poly-flex tubes.

Discharge Coefficient

The values of measured perforation flow rate are listed in Appendix B. The discharge coefficient was calculated for each measurement using the orifice formula. The average values of perforation discharge, discharge coefficient (C_Q), flow velocity, and Reynold's number for all the perforations were calculated and are summarized in Table 5. The range of average C_Q values was from 0.64 to 0.70 as compared with the theoretical value of 0.61 for sharp-edged orifices (Peterson, 1971). The relation between the measured discharge coefficient, and the calculated Reynold's number R was compared with the result published by Brater and King (1976). These measured values as compared with the practical values (Figure 12) show good agreement. The variation is from 2 to 5 percent.

Many factors can cause variability in the discharge coefficient. The most significant factor is probably the tube flow velocity as reported by Fry (1961). The discharge from the perforations is reduced as the velocity in the tube increases. Decreasing a perforation discharge means decreasing C_Q. This can be seen in Table 5 where the average C_Q for 0.5 inch tube was 0.64, but for the 1 inch tube it was

Table 5. Discharge Coefficient of Perforations

Tube Diameter in inches	Average Pressure in ft. of water	Orifice Diameter in inches 1/16	5/64	1/8	Average C_Q	R
	2	.6669	.6234	.6263		
	4	.6665	.6289	.6229		
1/2	6	.6814	.6231	.6171		
	8	.6767	.6248	.6150		
	10	.6759	.6327	.6181		
		.6735	.6266	.6199	.64	6,594
	2	.6817	.6620	.7102		
	4	.6795	.6537	.6812		
3/4	6	.6664	.6520	.6730		
	8	.6956	.6515	.6687		
	10	.6775	.6408	.6671		
		.6801	.6520	.6800	.67	7,834
	2	.6594	.7052	.7417		
	4	.6557	.7087	.7471		
1	6	.6575	.7077	.7336		
	8	.6316	.7206	.7418		
	10	.6319	.7143	.7333		
		.6472	.7113	.7395	.70	8,195

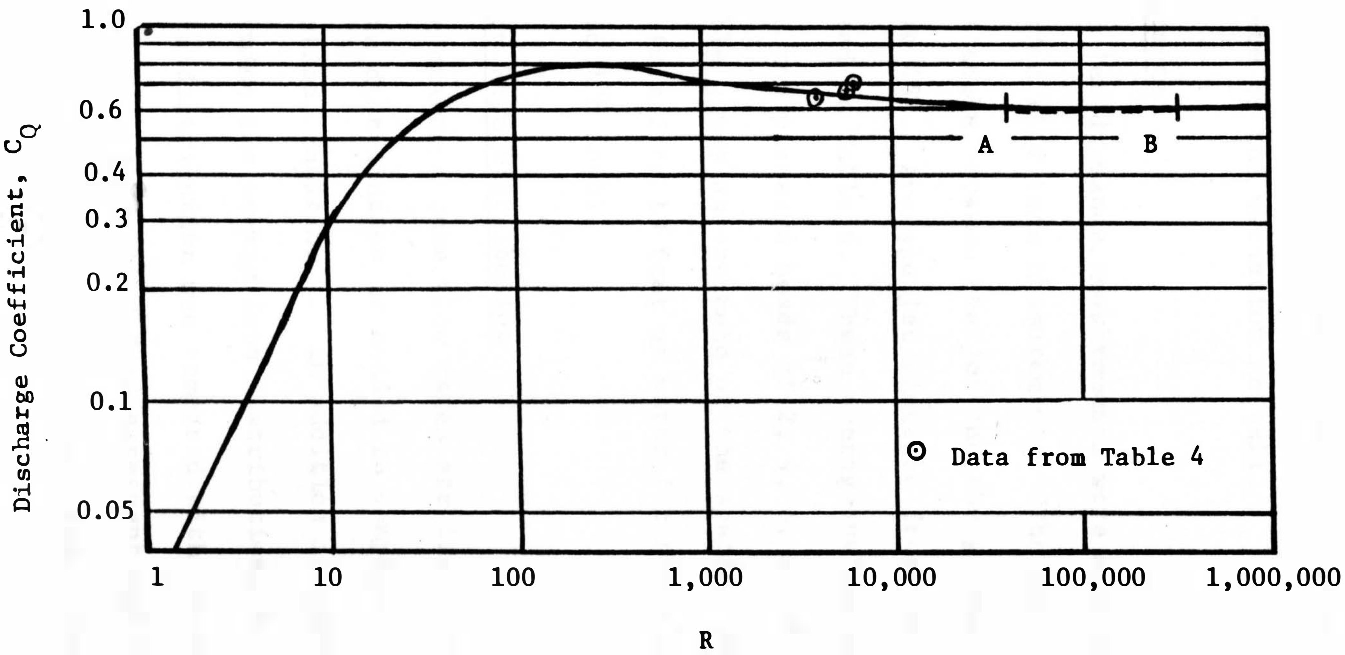

Figure 12: Values of Discharge Coefficient and Reynold's Number, R.

(Adapted from Brater and King, 1976).

0.70.

Other factors, such as the ratios of the perforation diameter to the tube wall thickness, the sharpness of the perforations' edge, and the smoothness of the inner surface (Brater and King, 1976) may contribute to the variation as well.

Jet Distance

The jet distance measurements were made in conjunction with the perforation flow rate measurements. The poly-flex tube was oriented so that the angle between the jet and the ground surface at the perforation is 45^{o}. Average jet distance from the ten perforations was summarized in Table 6. These average values are 2.8, 5.4, 8.0 and 9.8 feet for the pressure heads of 2, 4, 6, and 8 feet of water, respectively This table gives an estimate of the spacing to be covered with pressures ranging from 2 to 10 feet of water for three perforation sizes (1/16, 5/64, and 1/8 inch).

Tube Flow Rate Distribution

The measured tube flow rates are listed in Table 7. The tube flow rate distribution is needed to compare with the theoretical distribution, Equation 1. In addition it provides the basic information to determine the energy loss distribution, Equation 10. The measured flow rate distribution was compared with the theoretical flow rate distribution, Figure 13. Good agreement was obtained between the theoretical result and the measured data. The maximum variation is about 2.4 percent.

Table 6. Average Measured Jet Distance

Average Pressure Head Feet	1 Inch Tube, Orifice Size, Inch				3/4 Inch Tube, Orifice Size, Inch				1/2 Inch Tube, Orifice Size, Inch				Average x
	1/16 x	5/64 x	1/8 x	Average x	1/16 x	5/64 x	1/8 x	Average x	1/16 x	5/64 x	1/8 x	Average x	
2	3.3	2.5	3.3	3	2.5	2.5	2.5	2.5	2.5	2.8	3.3	2.8	2.8
4	5.8	4.5	6.6	5.6	5.0	4.2	4.8	4.6	5.4	6.0	6.6	6.0	5.4
6	8.3	7.1	10.8	8.8	6.6	6.6	6.6	6.6	8.0	8.3	10.0	8.7	8.0
8	10.8	8.7	12.5	10.6	8.3	8.3	9.0	8.5	10.0	10.8	- -	10.4	9.8
10	- -	- -	10.5	- -	10.0	10.0	10.0	10.0	- -	- -	- -	- -	- -

Where x = jet distance in feet

(angle between jet and ground surface at the perforation is 45^{o})

Table 7. Measured Orifices Flow Rate and Tube Flow Rate Distribution

$\frac{x}{L}$	ORIFICE NUMBER	ORIFICE FLOW RATE GPM	TUBE FLOW RATE GPM	$\frac{Q_x}{Q_0}$	VELOCITY FPS	$\frac{V^2}{2g}$ FEET
1.0	1	0.1188	0.1188	0.0	0.0	0.0
	2	0.1641	0.2829			
	3	0.1710	0.4539			
	4	0.1877	0.6416			
	5	0.1958	0.8374			
.75	6	0.1640	1.0014	0.1728	0.1728	0.00805
	7	0.1968	1.1982			
	8	0.1958	1.3940			
	9	0.1500	1.5440			
	10	0.1368	1.6808			
	11	0.1756	1.8564			
0.50	12	0.1257	1.9821	0.3419	1.42	0.0316
	13	0.1609	2.1430			
	14	0.1404	2.2834			
	15	0.1474	2.4308			
	16	0.2041	2.6349			
	17	0.1806	2.8155			
0.30	18	0.1417	2.9572	0.5102	2.13	0.0702
	19	0.1610	3.1182			
	20	0.1848	3.3030			
	21	0.1831	3.4861			
	22	0.1673	3.6534			
	23	0.1705	3.8239			
	24	0.1382	3.9621			
0.10	25	0.1638	4.1259	0.7118	2.97	0.137
	26	0.1713	4.2972			
	27	0.1505	4.4477			
	28	0.1706	4.6183			
	28	0.1706	4.6183			
	29	0.2072	4.8255			
	30	0.2052	5.0312			
	31	0.1743	5.2055			
	32	0.1978	5.4033			
	33	0.2126	5.6159			
0.0	34	0.1806	5.7965	1.0	4.17	0.27

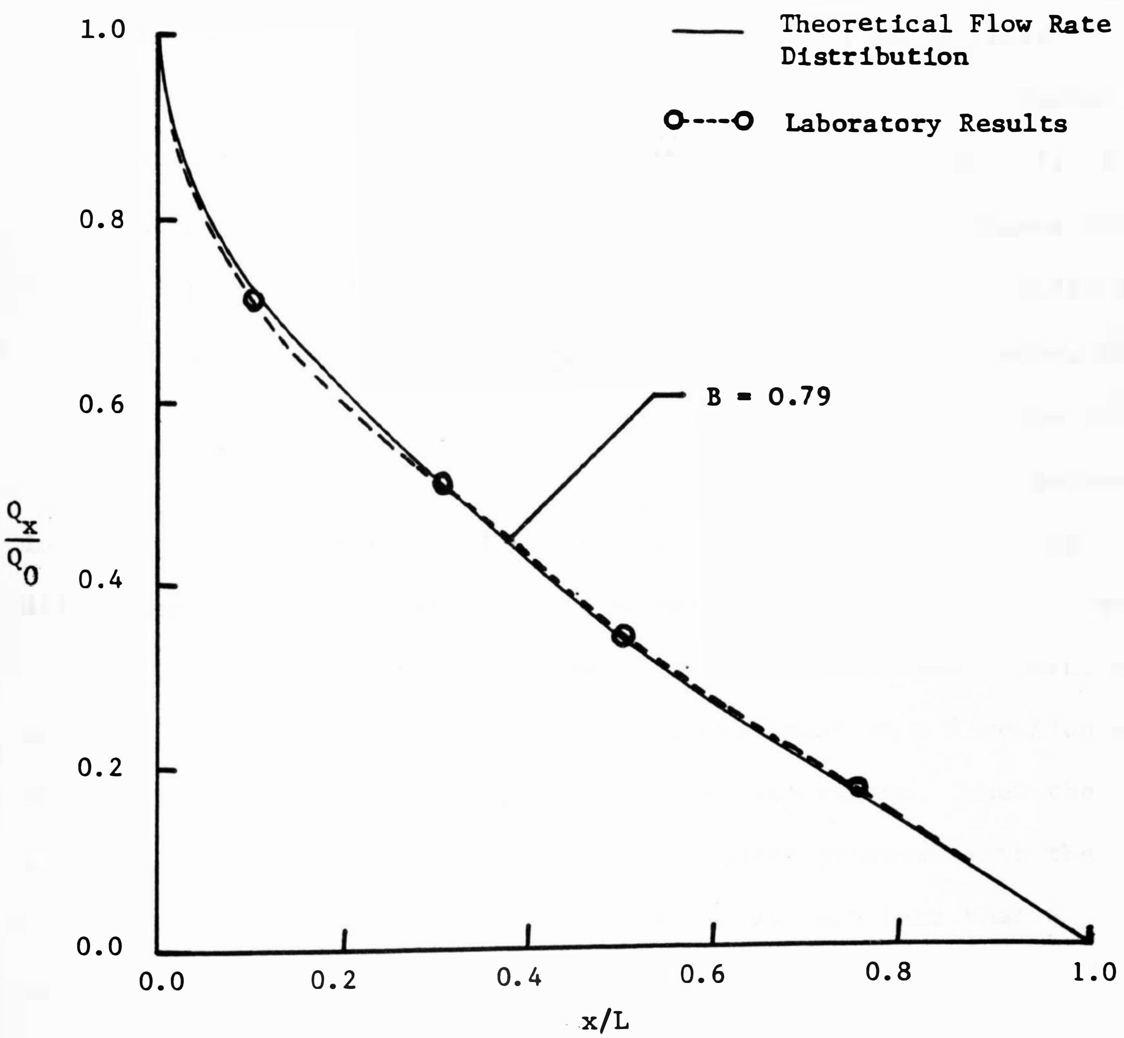

Figure 13: Dimensionless Distribution of Tube Flow Rate; Symbols Defined in Equation 8.

Energy Loss Distribution

The measured pressure head, elevation, velocity head of water flow at the six manometers on the tube are listed in Table 8. These input data were used to calculate the dimensionless energy loss distribution along the tube. The measured energy loss distribution is compared with the theoretical energy loss distribution, Table 8. A graphical comparison of the two distributions is shown in Figure 14. The discrepancy at the tube length ratio 0.0, 0.1, 0.3, 0.5, 0.75, and 1.0 is 0.0, 4.0, 17.0, 41.0, 70.0, and 0.0 percent, respectively, of the measured data values. The flow rate near the downstream end of the tube is usually small, and the Hazen-Williams formula may become inadequate to describe friction loss under such a condition. The discrepancy observed in the laboratory may be attributed to this cause.

Although the observed deviations between measured and theoretical energy loss distributions appears to be significant on a dimensionless basis, Figure 14, it was of little practical importance. When the deviation was examined by comparing the measured pressure with the calculated pressure from the theory, the errors were less than 6 percent, which is practically negligible, Table 8.

Table 8. The Measured and the Theoretical Energy Loss Distributions.

	Measured Values		Calculated Values				Theoretical Values				
$\frac{X}{L}$	P/γ	Z	$V^2/2g$	T.H.	H_f	H	H*	$(H_x - H_L)$	H_x		P/γ
	in.	in.	in.	in.	ft.			ft.	ft.	in.	in.
0.00	67.3200	0.0000	3.2400	70.5600	1.0674	1.0000	1.000	0.99	5.61	67.44	64.20
0.10	56.0000	0.0006	1.6400	66.6406	0.7407	0.6940	0.665	0.66	5.28	63.36	61.72
0.30	61.3125	0.0319	0.8430	62.1874	0.3697	0.3464	0.289	0.29	4.91	58.92	58.05
0.50	59.6250	-.0306	0.3790	59.9734	0.1852	0.1735	0.102	0.10	4.72	56.64	56.29
0.75	58.3125	-.0201	0.0966	58.3890	0.0532	0.0498	0.015	0.02	4.64	55.68	55.60
1.00	56.8125	0.9381	0.0000	59.7506	0.0000	0.0000	0.000	0.00	4.62**	55.44	54.50

$V^2/2g$ from Table 7.

T.H. - total head along the tube.

H_f - energy loss calculated by using Bernolli's equation.

H - calculated by using equation 10, ($H = H_x/H_0$, $H_0 = 1.0674$ ft).

H* - values from Figure 3, B = 0.79.

$(H_x - H_L)$ - shows the energy loss distribution along the tube.

H_x - the theoretical energy loss distribution along the tube.

** - from page 24, 4.62 ft = 2 psi.

P/γ - the theoretical pressure distribution = $[H_x - (\frac{V^2}{2g} + Z)]$, Z = potential head.

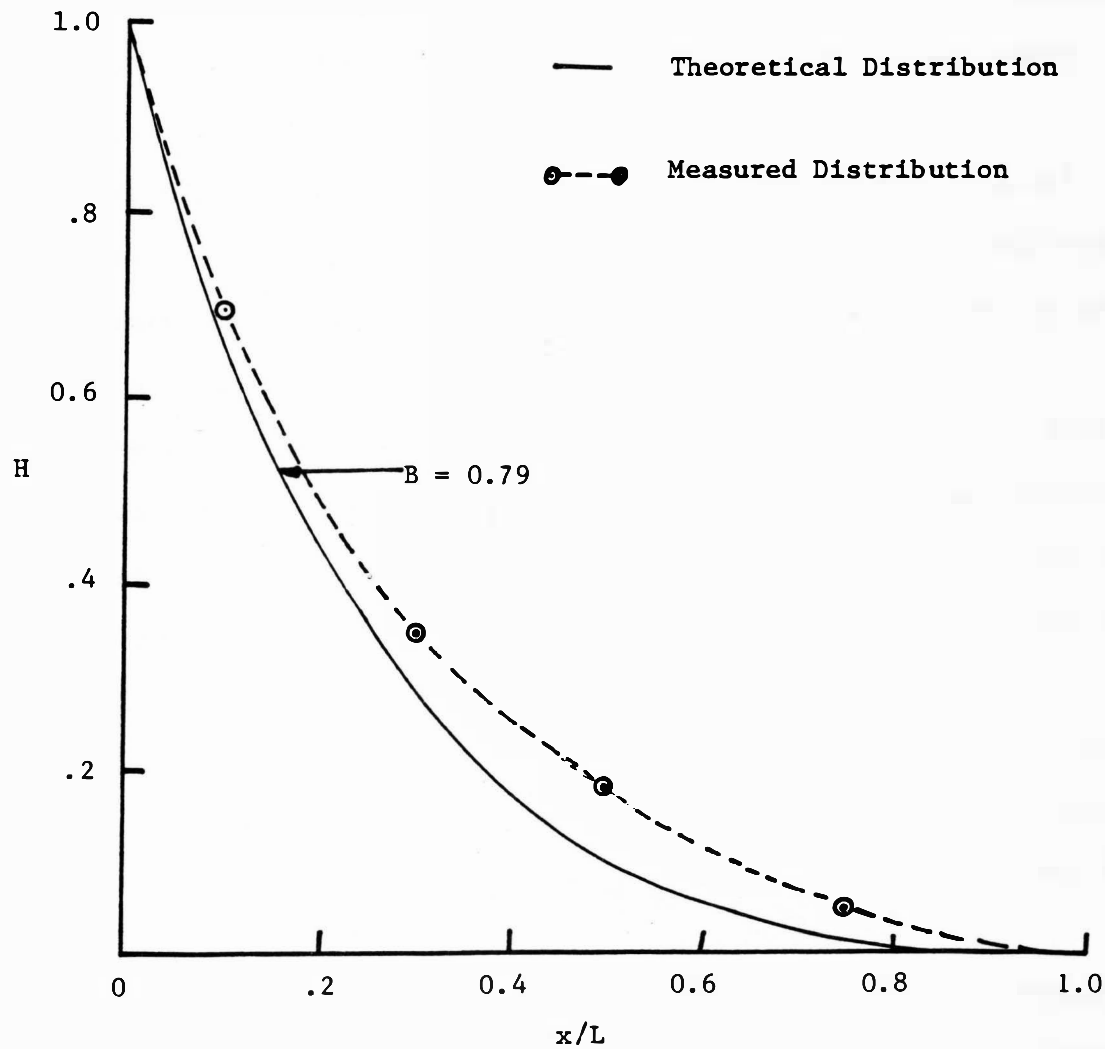

Figure 14: Measured and Theoretical Energy Loss Distribution; Symbols Defined in Equations 10 and 8.

SUMMARY AND CONCLUSIONS

The friction coefficients of poly-flex tubes, the discharge coefficients of perforations along a trail tube, and the jet distances of water distributed by trail tubes were determined by laboratory measurements.

The Hazen-Williams formula was found to be an adequate model to describe friction loss of poly-flex tubes. Friction loss coefficients of measured data based upon Hazen-Williams formula were found to be within a range of 130 to 135.

The discharge coefficients for perforations with sizes of 1/16, 5/64, and 1/8 inch were determined. It was found that the perforation size has little effect on the discharge coefficient but tube size has an effect. The discharge coefficient values were 0.64, 0.67, and 0.7 for tube sizes of 1/2, 3/4 and 1 inch, respectively.

Jet distances for perforation sizes of 1/16, 5/64, and 1/8 inch under different pressures were measured. Perforation size has little effect on jet distance, but operating pressure has a major effect on jet distance.

Laboratory data were used to evaluate a theory of tube irrigation developed by Chu (1982). This theory was tested for the conditions of the outermost trail-tube on a center pivot system. The tube was located at 1318 feet away from the pivot. It was to apply 1 inch of water in a period of 3 days on a 1.0 intake family soil. The tube spacing and perforation size were selected to be 5 feet and 5/64 inches. An operating pressure of 2 pounds per square inch was selected for the downstream end of the tube.

Under the above conditions, perforation spacings were calculated according to the theory. Thirty-four perforations were drilled in a 3/4 inch poly-flex tube based upon the calculated spacings. The flow rate from these perforations and the pressure along the tube of 38 feet in length were measured. Comparisons of these measurements with the theoretical flow rate and the energy loss distribution indicated that

1. The measured discharge distribution was in good agreement with the theory.

2. The measured energy loss distribution was also in good agreement with the theory in general but deviations between the measured and the theoretical distributions were observed near the downstream end of the tube.

Tube discharge near the downstream end is usually small (laminar flow); the Hazen-Williams formula probably is inadequate to represent the friction loss under such a condition. The observed deviation may be attributed to the existence of laminar flow at the downstream end of the tube.

The deviation between measured and theoretical energy loss distribution appeared to be significant on a dimensionless basis. But when this deviation was examined by comparing the measured pressure with the theoretical pressure the errors were less than 6 percent and would be negligible in practice.

References

Brater and King. 1976. Handbook of Hydraulics. Sixth Edition. McGraw-Hill Book Company, New York. Sections (Sec.) and Pages (p.). (Sec. 1, p. 8; Sec.4, p. 1, 3, 6-8; 29, Sec. 6, p. 3, 9, 10, 11, 17).

Christiansen, J. E. 1942. Irrigation by Sprinklers, Bulletin 670. University of California. p. 64-67.

Christiansen, J. E. and J. R. Davis. 1967. Sprinkler Irrigation Systems, p. 885-904. In Hagan, R. M., H. R. Haise, and T. W. Edminster. (Eds.) 1967. Irrigation of Agricultural Lands. Monograph no. 11, American Society of Agronomy, Madison, Wisc. p. 895.

Chu, S. T. 1982. Analysis of Irrigation by Trail Tubes. American Society of Agricultural Engineering. Paper no. 2003, SDSU, Brookings, SD.

Chu, S. T. and D. L. Moe. 1972. Hydraulics of a Center Pivot System. Trans. of the ASAE 15(5):894-896.

Fry, A. W. 1961. Discharge from Gated Pipe. College of Agriculture, University of California, Agricultural Experimental Service.

Hanks, R. J., G. L. Ashcroft. (Eds.) 1980. Applied Soil Physics. Spring-Verlag. NY. p. 78-80.

Hart, W. E. 1980. Design and Operation of Gravity or Surface Systems. p. 501-580. In Design and Operation of Farm Irrigation Systems. Edited by M. E. Jenson. ASAE Monograph no. 3, p. 502-503.

Howell, T. A., C. J. Phene and D. C. Sandres. 1980. A New Concept for Trickle Irrigation of Raw Crops. Drip/Trickle Irrigation, Winter 1980, p. 18-20.

Howell, T. A., F. K. Aljibury, H. M. Gitlin, I-Pai Wu, A. W. Warrick and P. A. C. Raats. 1980. Design and Operation of Trickle (Drip) Systems, p. 663-717. In Design and Operation of Farm Irrigation Systems. Edited by M. E. Jenson. ASAE Monograph no. 3, p. 663-665.

Medaugh, F. W. and G. D. Johnson. 1940. Investigation of the Discharge and Coefficients of Small Circular Orifices. ASCE 10(7):422-424.

Merrian, J. L. 1968. Irrigation System Evaluation and Improvement. Black Printery, San Luis obispo, CA. p. 4.

Moody, L. F. 1944. Friction Factors for Pipe Flow, Trans. ASME, Vol. 66, p. 671. November, 1944.

References Continued

Pair, C. H., W. W. Hinz, C. Reid, and K. R. Frost. 1975. Sprinkler Irrigation. Sprinkler Irrigation Association, Silver Spring, MD. p. 231-232.

Peterson, A. C. 1971. Applied Mechanics: Fluids. Allyn and Bacon, Inc. Boston, MA. p. 152.

Philip, J. R. 1957. The Theory of Infiltration: 4. Sorptivity and Algebraic Infiltration Equations. Soil Sci. 84:257-264.

Rawlins, S. L., G. J. Hoffman, and S. D. Merril. 1979. Traveling Trickle System. Proc., Second International Irrigation Congress, San Diego, CA. p. 184-187.

Scorborough, J. B. 1955. Numerical Mathematical Analysis. Third Edition, The Johns Hopkins Press. p. 132.

Schwab, O. G., R. K. Frevert, T. W. Edminster and K. K. Barnes. 1966. Soil and Water Conservation Engineering. Second Edition. John Wiley and Sons, NY. p. 122, 587.

Soil Conservation Service (SCS, USDA). 1964. Soil-Plant-Water Relationships. National Engineering Hanbook, Section 15, Chapter 1, p. 17, 24-26.

Steel, R. G. D., J. H. Torrie. 1980. Principles and Procedures of Statistics. Second Edition. McGraw-Hill Company. NY. p. 27.

Vennard, J. K. 1961. Elementary Fluid Mechanics, Fourth Edition, John Wiley and Sons, Inc. NY. p. 283-284.

Villemonte, J. R. 1977. Some Basic Concepts on Flow in Branching Conduits. ASCE, Vol, 103, No. HY7, July 1977. University of Wisconsin, Madison, WI.

Wu, I-Pai, T. A. Howell and E. A. Hiler. 1979. Hydraulic Design of Drip Irrigation Systems. Tech. Bull. No. 105, Hawaii Agricultural Experimental Station, University of Hawaii, HA.

APPENDIXES

APPENDIX A

Friction Coefficient Data

SYMBOLS USED IN APPENDIX A

H_1 = the pressure at the upstream side of the tube in feet of water

H_2 = the pressure at the downstream side of the tube in feet of water

GPM = gallons per minute

FPS = feet per second

$V^2/2g$ = velocity head

H_f, f, c, and K_s, see equations 1, 2, and 3.

R = Reynold's number (at $60^{\circ}F$), for tubes.

Table A: Measured Friction Loss and Calculated Friction Coefficients

Tube size inch	H_1 feet	H_2 feet	H_f ft/L	Dis-charge GPM	Velo-city V FPS	$V^2/2g$ feet	Friction Coefficients f	C	K_s	R
1/2	4.7377	4.6023	0.1354	0.5111	0.6852	0.0073	0.0341	145.00	0.3747	02,590
(L=25	0.9043	0.4148	0.4896	0.8829	1.1836	0.0218	0.0413	125.00	0.4795	04.474
feet)	1.0710	0.4877	0.5833	0.9847	1.3201	0.0271	0.0396	127.00	0.4643	04,990
	1.9043	0.9981	0.9063	1.3533	1.8143	0.0512	0.0326	138.00	0.3943	06,858
	2.0710	0.9460	1.1250	1.3704	1.8372	0.0525	0.0394	124.00	0.4779	06,944
	3.9043	1.9668	1.9375	1.9432	2.6051	0.1055	0.0338	131.00	0.4239	09,847
	4.0710	1.9460	2.1250	1.9733	2.6455	0.1088	0.0359	127.00	0.4515	09,999
	5.9043	2.9252	2.9792	2.4141	3.2364	0.1629	0.0337	129.00	0.4316	12,233
	6.1127	3.0293	3.0834	2.4342	3.2634	0.1656	0.0343	128.00	0.4397	12,335
	7.9043	4.0085	3.8958	2,8170	3.7766	0.2217	0.0323	130.00	0.4209	14,275
	8.4043	4.2795	4.1250	2.9039	3.8931	0.2356	0.0322	130.00	0.4207	14,715
	9.9043	5.0814	4.8229	3.1676	4.2466	0.2804	0.0316	131.00	0.4170	16,051
							0.0351	130.35	0.4330	
3/4	0.9949	0.2631	0.7318	1.8010	1.2954	0.0261	0.0350	131.75	0.4248	06,685
(L=50	1.9949	0.3360	1.6589	2.8472	2.0480	0.0652	0.0320	133.89	0.4037	10,568
feet)	3.9949	0.5652	3.4292	4.1950	3.0174	0.1416	0.0300	133.26	0.3997	15,570
	5.9949	0.3465	5.6484	5.6724	4.0801	0.2588	0.0272	137.64	0.3711	21,054
	8.9949	2.2631	6.7318	6.1853	4.4490	0.3077	0.0274	136.52	0.3752	22,958
	7.9949	0.5808	7.4141	6.5422	4.7058	0.3443	0.0270	137.06	0.3714	24,283
	9.9949	0.5652	9.4297	7.3801	5.3085	0.4381	0.0270	135.79	0.3757	27,393
							0.0294	135.13	0.3888	
1.0	2.0287	0.7631	1.2656	5.6242	2.1393	0.0712	0.0307	132.42	0.4025	15,180
(L=50	4.0287	1.6798	2.3490	7.9815	3.0360	0.1433	0.0283	134.58	0.3841	21,543
feet)	6.0287	2.6329	3.3958	9.8360	3.7414	0.2176	0.0270	135.92	0.3734	26,549
	8.0287	3.5808	4.4479	11.4549	4.3572	0.2952	0.0260	136.82	0.3661	30,919
	10,0287	4.0704	5.9583	12.9115	4.9113	0.3750	0.0274	131.70	0.4620	34,850
							0.0279	134.29	0.3144	

APPENDIX B

Measured Perforation Flow Rate and Calculated Discharge Coefficient

SYMBOLS USED IN APPENDIX B

H_1 = the pressure at the upstream side of the tube

H_2 = the pressure at the downstream side of the tube

H = average pressure

C_Q = the discharge coefficient

V = average velocity of flow of orifices in ft/sec

R = Reynold's number (at t = 60^{o}F), for orifices

Note:
- Some values are eliminated from 1/2 and 3/4 inch tubes because of either too large or too small perforations (total perforations were 10).
- Values between parenthesis are averages.

Table B1: Measured Perforation Flow Rate and Calculated Discharge Coefficient

Tube size inch	Orifice size inch	Orifice number	H_1 inch	H_2 inch	Average H inch	Discharge GPM	C_Q	Average V FPS	R
1/2	1/16	1	24.079	23.954	24.0165	0.0567	0.5235		
		2				0.0826	0.7626		
		3				0.0863	0.7968		
		4				0.0770	0.7109		
		5				0.0726	0.6703		
		6				0.0704	0.6500		
		7				0.0600	0.5539		
						(0.0776)	(0.6669)	8.12	3,467
		1	48.079	47.954	48.0165	0.0802	0.5237		
		2				0.1159	0.7568		
		3				0.1191	0.7777		
		4				0.0986	0.6438		
		5				0.1085	0.7084		
		6				0.1033	0.6745		
		7				0.0896	0.5809		
						(0.1021)	(0.6665)	10.68	4,562
		1	72.079	71.954	72.0165	0.0982	0.5236		
		2				0.1433	0.7640		
		3				0.1451	0.7736		
		4				0.1347	0.7182		
		5				0.1337	0.7128		
		6				0.1286	0.6856		
		7				0.1110	0.5918		
						(0.1278)	(0.6814)	13.36	5,711

Table B1: Continued.

Tube size inch	Orifice size inch	Orifice number	H_1 inch	H_2 inch	Average H inch	Discharge GPM	C_Q	Average V FPS	R
		1	96.079	95.954	96.0165	0.1127	0.5204		
		2				0.1641	0.7577		
		3				0.1569	0.7245		
		4				0.1562	0.7212		
		5				0.1551	0.7162		
		6				0.1519	0.7014		
		7				0.1289	0.5952		
						(0.1465)	(0.6767)	15.32	6,546
		1	120.079	119.954	120.0165	0.1254	0.5179		
		2				0.1888	0.7797		
		3				0.1836	0.7583		
		4				0.1752	0.7237		
		5				0.1573	0.6497		
		6				0.1723	0.7116		
		7				0.1429	0.5902		
						(0.1636)	(0.6759)	17.11	7,310
1/2	5/64	1	24.079	23.954	24.0165	0.1032	0.6092		
		2				0.1136	0.6706		
		3				0.1033	0.6098		
		4				0.1134	0.6694		
		5				0.1012	0.5974		
		6				0.1089	0.6428		
		7				0.0957	0.5649		
						(0.1056)	(0.6234)	7.07	3,775

Table B1: Continued.

Tube size inch	Orifice size inch	Orifice number	H_1 inch	H_2 inch	Average H inch	Discharge GPM	C_Q	Average V FPS	R
		1	48.079	47.954	48.0165	0.1439	0.6008		
		2				0.1618	0.6755		
		3				0.1503	0.6275		
		4				0.1570	0.6555		
		5				0.1438	0.6003		
		6				0.1598	0.6671		
		7				0.1379	0.5757		
						(0.1506)	(0.6289)	10.08	5,383
		1	72.079	71.954	72.0165	0.1769	0.6030		
		2				0.1909	0.6508		
		3				0.1812	0.6177		
		4				0.1937	0.6603		
		5				0.1754	0.5979		
		6				0.1929	0.6576		
		7				0.1684	0.5741		
						(0.1828)	(0.6231)	12.23	6,534
		1	96.079	95.954	96.0165	0.2042	0.6029		
		2				0.2207	0.6518		
		3				0.2100	0.6200		
		4				0.2222	0.6560		
		5				0.2006	0.5922		
		6				0.2258	0.6666		
		7				0.1979	0.5843		
						(0.2116)	(0.6248)	14.16	7,564

Table B1: Continued.

Tube size inch	Orifice size inch	Orifice number	H_1 inch	H_2 inch	Average H inch	Discharge GPM	C_Q	Average V FPS	R
		1	120.079	119.954	120.0165	0.2308	0.6095		
		2				0.2518	0.6649		
		3				0.2308	0.6095		
		4				0.2556	0.6750		
		5				0.2312	0.6105		
		6				0.2498	0.6596		
		7				0.2272	0.6000		
						(0.2396)	(0.6327)	16.04	8,565
1/2	1/8	1	23.8915	23.7665	23.8290	0.2594	0.6001		
		2				0.2664	0.6163		
		3				0.2552	0.5904		
		4				0.2705	0.6258		
		5				0.2913	0.6739		
		6				0.2928	0.6774		
		7				0.2594	0.6001		
						(0.2707)	(0.6263)	7.08	6,048
		1	47.8915	47.7665	47.8290	0.3572	0.5833		
		2				0.3677	0.6004		
		3				0.3626	0.5921		
		4				0.3859	0.6302		
		5				0.4091	0.6680		
		6				0.4157	0.6788		
		7				0.3720	0.6075		
						(0.3815)	(0.6229)	9.97	8,523

Table B1: Continued.

Tube size inch	Orifice size inch	Orifice number	H_1 inch	H_2 inch	Average H inch	Discharge GPM	C_Q	Average V FPS	R
		1	71.8915	71.7665	71.8290	0.4258	0.5674		
		2				0.4439	0.5915		
		3				0.4403	0.5867		
		4				0.4674	0.6228		
		5				0.4993	0.6653		
		6				0.5084	0.6774		
		7				0.4569	0.6088		
						(0.4631)	(0.6171)	12.11	10,346
		1	95.8915	95.7665	95.8290	0.4971	0.5735		
		2				0.5123	0.5910		
		3				0.5067	0.5845		
		4				0.5324	0.6142		
		5				0.5773	0.6660		
		6				0.5807	0.6699		
		7				0.5253	0.6060		
						(0.5331)	(0.6150)	13.94	11,910
		1	119.8915	119.7665	119.8290	0.4997	0.5155		
		2				0.5824	0.6008		
		3				0.6286	0.6485		
		4				0.5933	0.6121		
		5				0.6516	0.6722		
		6				0.6417	0.6620		
		7				0.5965	0.6154		
						(0.5991)	(0.6181)	15.66	13,385

Table B2: Measured Perforation Flow Rate and Calculated Discharge Coefficient

Tube size inch	Orifice size inch	Orifice number	H_1 inch	H_2 inch	Average H inch	Discharge GPM	C_Q	Average V FPS	Average R
3/4	1/16	1	24.3775	24.2838	24.3306	0.0712	0.6194		
		2				0.0905	0.7873		
		3				0.0685	0.5959		
		4				0.0798	0.6943		
		5				0.0693	0.6029		
		6				0.0834	0.7256		
		7				0.0858	0.7465		
						(0.0784)	(0.6817)	8.20	3,503
		1	48.3775	48.2838	48.3306	0.1226	0.7568		
		2				0.1241	0.7660		
		3				0.1013	0.6253		
		4				0.0983	0.6068		
		5				0.1016	0.6272		
		6				0.1113	0.6870		
		7				0.1114	0.6871		
						(0.1184)	(0.6795)	12.38	5,291
		1	74.3775	72.2838	76.3306	0.1507	0.7402		
		2				0.1319	0.6479		
		3				0.1169	0.5742		
		4				0.1206	0.5924		
		5				0.1503	0.7383		
		6				0.1370	0.6729		
		7				0.1423	0.6990		
						(0.1357)	(0.6664)	14.19	6,064

Table B2: Continued.

Tube size inch	Orifice size inch	Orifice number	H_1 inch	H_2 inch	Average H inch	Discharge GPM	C_Q	Average V FPS	R
		1	96.3775	96.2838	96.3306	0.1423	0.6222		
		2				0.1570	0.6865		
		3				0.1671	0.7306		
		4				0.1588	0.6943		
		5				0.1399	0.6117		
		6				0.1698	0.7424		
		7				0.1787	0.7813		
						(0.1591)	(0.6956)	16.64	7,109
		1	120.3775	120.2838	120.3306	0.1532	0.5993		
		2				0.1840	0.7198		
		3				0.1837	0.7186		
		4				0.1746	0.6830		
		5				0.1535	0.6005		
		6				0.1712	0.6697		
		7				0.1921	0.7515		
						(0.1732)	(0.6775)	18.11	7,739
3/4	5/64	1	24.1588	24.0650	24.1119	0.1142	0.6728		
		2				0.1065	0.6274		
		3				0.1129	0.6651		
		4				0.1051	0.6192		
		5				0.1186	0.6987		
		6				0.1258	0.7411		
		7				0.1035	0.6098		
						(0.1124)	(0.6620)	7.53	4,018

Table B2: Continued.

Tube size inch	Orifice size inch	Orifice number	H_1 inch	H_2 inch	Average H inch	Discharge GPM	C_Q	Average V FPS	R
		1	48.1588	48.0650	48.1119	0.1602	0.6681		
		2				0.1464	0.6106		
		3				0.1564	0.6523		
		4				0.1475	0.6152		
		5				0.1656	0.6907		
		6				0.1733	0.7228		
		7				0.1477	0.6160		
						(0.1567)	(0.6537)	10.49	5,601
		1	72.1588	72.0650	72.1119	0.1955	0.6660		
		2				0.1780	0.6064		
		3				0.1908	0.6500		
		4				0.1802	0.6139		
		5				0.2018	0.6875		
		6				0.2128	0.7249		
		7				0.1806	0.6152		
						(0.1914)	(0.6520)	12.81	6,842
		1	96.1588	96.0650	96.1119	0.2275	0.6713		
		2				0.2040	0.6020		
		3				0.2200	0.6492		
		4				0.2085	0.6153		
		5				0.2336	0.6893		
		6				0.2476	0.7306		
		7				0.2043	0.6029		
						(0.2124)	(0.6515)	14.22	7,592

Table B2: Continued.

Tube size inch	Orifice size inch	Orifice number	H_1 inch	H_2 inch	Average H inch	Discharge GPM	C_Q	Average V FPS	Average R
		1	120.1588	120.0650	120.1119	0.2270	0.5992		
		2				0.2273	0.6000		
		3				0.2451	0.6470		
		4				0.2328	0.6145		
		5				0.2600	0.6863		
		6				0.2769	0.7309		
		7				0.2301	0.6074		
						(0.2427)	(0.6408)	16.24	8,675
3/4	1/8	1	24.1275	24.0337	24.0805	0.2889	0.6649		
		2				0.3241	0.7459		
		3				0.2919	0.6718		
		4				0.3223	0.7417		
		5				0.3147	0.7242		
		6				0.3038	0.6992		
		7				0.3144	0.7235		
						(0.3086)	(0.7102)	8.07	6,895
		1	48.1275	48.0337	48.0806	0.4002	0.6518		
		2				0.4581	0.7461		
		3				0.4171	0.6934		
		4				0.3873	0.6308		
		5				0.4003	0.6520		
		6				0.4233	0.6894		
		7				0.4290	0.7051		
						(0.4232)	(0.6812)	11.06	9,455

Table B2: Continued.

Tube size inch	Orifice size inch	Orifice number	H_1 inch	H_2 inch	Average H inch	Discharge GPM	C_Q	Average V FPS	R
		1	72.1275	72.0337	72.0806	0.4851	0.6453		
		2				0.5586	0.7430		
		3				0.5029	0.6690		
		4				0.4754	0.6324		
		5				0.4810	0.6399		
		6				0.5113	0.6801		
		7				0.5271	0.7011		
						(0.5059)	(0.6730)	13.23	11,303
		1	96.1275	96.0337	96.0806	0.5582	0.6431		
		2				0.6350	0.7316		
		3				0.5860	0.6751		
		4				0.5386	0.6206		
		5				0.5562	0.6408		
		6				0.5823	0.6709		
		7				0.6067	0.6990		
						(0.5804)	(0.6687)	15.17	12,967
		1	120.1275	120.0337	120.0806	0.6287	0.6479		
		2				0.6957	0.7170		
		3				0.6637	0.6840		
		4				0.6014	0.6198		
		5				0.6245	0.6436		
		6				0.6457	0.6654		
		7				0.6718	0.6923		
						(0.6473)	(0.6671)	16.92	14,462

Table B3: Measured Perforation Flow Rate and Calculated Discharge Coefficient

Tube size inch	Orifice size inch	Orifice number	H_1 inch	H_2 inch	Average H inch	Discharge GPM	C_Q	Average V FPS	R
1.0	1/16	1	24.5015	24.439	24.4703	0.0753	0.6887		
		2				0.0655	0.5991		
		3				0.0827	0.7564		
		4				0.0739	0.6759		
		5				0.0770	0.7043		
		6				0.0752	0.6878		
		7				0.0713	0.6521		
		8				0.0688	0.6293		
		9				0.0741	0.6777		
		10				0.0575	0.5259		
						(0.0721)	(0.6594)	7.54	3,222
		1	48.5015	48.4390	48.4703	0.1036	0.6733		
		2				0.0899	0.5842		
		3				0.1152	0.7487		
		4				0.1037	0.6739		
		5				0.1075	0.6986		
		6				0.1061	0.6895		
		7				0.0959	0.6232		
		8				0.1032	0.6707		
		9				0.1032	0.6707		
		10				0.0806	0.5238		
						(0.1009)	(0.6557)	10.55	4,509
		1	72.4975	72.4350	74.4663	0.1257	0.6681		
		2				0.1404	0.7462		
		3				0.1398	0.7430		
		4				0.1188	0.6314		
		5				0.1343	0.7138		

Table B3: Continued.

Tube size inch	Orifice size inch	Orifice number	H_1 inch	H_2 inch	Average H inch	Discharge GPM	C_Q	Average V FPS	R
		6				0.1281	0.6809		
		7				0.1148	0.6102		
		8				0.1134	0.6027		
		9				0.1251	0.6649		
		10				0.0971	0.5161		
						(0.1237)	(0.6575)	12.94	5,527
		1	96.435	96.535	96.4663	0.1440	0.6634		
		2				0.1251	0.5764		
		3				0.1622	0.7472		
		4				0.1436	0.6612		
		5				0.1314	0.6053		
		6				0.1483	0.6832		
		7				0.1307	0.6021		
		8				0.1302	0.5998		
		9				0.1440	0.6638		
		10				0.1115	0.5136		
						(0.1371)	(0.6316)	14.34	6,126
		1	120.4975	120.435	120.4663	0.1597	0.6583		
		2				0.1403	0.5784		
		3				0.1600	0.6596		
		4				0.1613	0.6649		
		5				0.1646	0.6785		
		6				0.1662	0.6851		
		7				0.1471	0.6064		
		8				0.1454	0.5994		
		9				0.1607	0.6625		
		10				0.1279	0.5272		
						(0.1533)	(0.6319)	16.03	6,850

Table B3: Continued.

Tube size inch	Orifice size inch	Orifice number	H_1 inch	H_2 inch	Average H inch	Discharge GPM	C_Q	Average V FPS	R
1.0	5/64	1	24.5015	24.4390	24.4703	0.1404	0.8206		
		2				0.1206	0.7047		
		3				0.1173	0.6858		
		4				0.1231	0.7192		
		5				0.1077	0.6292		
		6				0.1280	0.7480		
		7				0.1045	0.6105		
		8				0.1228	0.7179		
		9				0.1252	0.7315		
		10				0.1171	0.6844		
						(0.12067)	(0.7052)	8.08	4,313
		1	48.525	48.4390	48.4703	0.1936	0.8038		
		2				0.1684	0.6993		
		3				0.1615	0.6705		
		4				0.1684	0.6995		
		5				0.1595	0.6622		
		6				0.1832	0.7607		
		7				0.1479	0.6142		
		8				0.1812	0.7525		
		9				0.1794	0.7450		
		10				0.1636	0.6793		
						(0.17067)	(0.7052)	11.42	6,101
		1							
		1	72.5015	72.4390	72.4703	0.2323	0.7890		
		2				0.2045	0.6944		
		3				0.2045	0.6944		
		4				0.2032	0.6901		
		5				0.2003	0.6801		

Table B3: Continued.

Tube size inch	Orifice size inch	Orifice number	H_1 inch	H_2 inch	Average H inch	Discharge GPM	C_Q	Average V FPS	R
		6				0.2223	0.7549		
		7				0.1799	0.6110		
		8				0.2226	0.7559		
		9				0.2150	0.7302		
		10				0.1992	0.6765		
						(0.2084)	(0.7077)	13.95	7,449
		1	96.5015	96.4390	96.4703	0.2699	0.7943		
		2				0.2383	0.7015		
		3				0.2609	0.7679		
		4				0.2322	0.6834		
		5				0.2305	0.6784		
		6				0.2549	0.7503		
		7				0.2148	0.6322		
		8				0.2579	0.7590		
		9				0.2502	0.7365		
		10				0.2385	0.7021		
						(0.2448)	(0.7206)	16.38	8,751
		1	120.5015	120.4390	120.4703	0.3094	0.8150		
		2				0.2688	0.7080		
		3				0.3002	0.7907		
		4				0.2615	0.6888		
		5				0.2288	0.6027		
		6				0.2817	0.7420		
		7				0.2159	0.5687		
		8				0.3052	0.8039		
		9				0.2937	0.7736		
		10				0.2468	0.6501		
						(0.2712)	(0.7143)	18.15	9,694

Table B3: Continued.

Tube size inch	Orifice size inch	Orifice number	H_1 inch	H_2 inch	Average H inch	Discharge GPM	C_Q	Average V FPS	R
1.0	1/8	1	24.8140	24.7515	24.7828	0.3326	0.7545		
		2				0.3278	0.7436		
		3				0.3101	0.7035		
		4				0.3323	0.7538		
		5				0.3430	0.7781		
		6				0.3740	0.7810		
		7				0.3074	0.6973		
		8				0.3330	0.7554		
		9				0.2905	0.6590		
		10				0.3188	0.7232		
						(0.3270)	(0.7417)	8.55	7,306
		1	48.8140	48.7515	48.7828	0.4665	0.7573		
		2				0.4631	0.7488		
		3				0.4399	0.7113		
		4				0.4760	0.7697		
		5				0.4814	0.7784		
		6				0.4906	0.7933		
		7				0.4548	0.7354		
		8				0.4299	0.6951		
		9				0.4427	0.7158		
		10				0.4757	0.7692		
						(0.4621)	(0.7471)	12.08	10,324
		1	72.8140	72.7575	72.7828	0.5722	0.7574		
		2				0.5530	0.7320		
		3				0.5345	0.7075		
		4				0.5811	0.7692		
		5				0.5733	0.7589		

Table B3: Continued.

Tube size inch	Orifice size inch	Orifice number	H_1 inch	H_2 inch	Average H inch	Discharge GPM	C_Q	Average V FPS	R
		6				0.5951	0.7878		
		7				0.5295	0.7009		
		8				0.5252	0.6952		
		9				0.5232	0.6926		
		10				0.5551	0.7348		
						(0.5542)	(0.7336)	14.49	12,382
		1	96.814	96.7515	96.7828	0.6974	0.8006		
		2				0.6322	0.7257		
		3				0.5985	0.6870		
		4				0.6671	0.7658		
		5				0.6662	0.7648		
		6				0.6717	0.7711		
		7				0.6094	0.6996		
		8				0.6596	0.7572		
		9				0.5989	0.6875		
		10				0.6612	0.7590		
						(0.6462)	(0.7418)	16.89	14,437
		1	120.814	120.7515	120.7828	0.7380	0.7584		
		2				0.7013	0.7206		
		3				0.6295	0.6469		
		4				0.7529	0.7737		
		5				0.7510	0.7717		
		6				0.7587	0.7796		
		7				0.6527	0.6707		
		8				0.7425	0.7630		
		9				0.6830	0.7018		
		10				0.7268	0.7468		
						(0.7136)	(0.7333)	18.66	15,943

APPENDIX C

Numerical Solution of Equations 8, 9, and 10.

SYMBOLS USED IN

APPENDIX C

Where

$$f = [(1 + B\frac{x}{L}) - (B\frac{x}{L} + \frac{x}{L})]^{1.85}\ d(\frac{x}{L})$$

$$da = area = \frac{dx}{6}(y_0 + 4y_1 + y_2)$$

d_x = the interval of integration divided into an even number subinterval of width d_x.

y_0, y_1, y_2 = the only functional values in the above interval.

$H_x/H_f = \int_1^{x/L} (f)$, Equation 11 (Chu, 1982).

H = Energy loss distribution

$= \frac{1}{F}\int_1^{x/L} (f)$, (Equation 10).

F = F - Factor = the sum of da, (Equation 9).

Q_x/Q_0 = Discharge distribution along the tube, (Equation 8).

Table C1: Numerical Solution of Equations 8, 9, and 10.
B = 0

x/L	f	Simpson's factor	Product	$y_0+4y_1+y_2$	da	$\frac{H_x}{H_f}$	H	Q_x/Q_0
0.00	1.0000	1	1.0000			(0.3504)	1.0000	1.0000
0.05	0.9095	4	3.6380					0.9500
0.10	0.8229	1	0.8229	5.4609	0.0910	0.2594	0.7403	0.9000
0.15	0.7403	4	2.9612					0.8500
0.20	0.6618	1	0.6618	2.4459	0.0741	0.1853	0.5288	0.8000
0.25	0.5873	4	0.3492					0.7500
0.30	0.5169	1	0.5169	3.5279	0.0588	0.1265	0.3610	0.7000
0.35	0.4507	4	1.8028					0.6500
0.40	0.3887	1	0.3887	2.7084	0.0451	0.0814	0.2323	0.6000
0.45	0.3309	4	1.3236					0.5500
0.50	0.2774	1	0.2774	1.9897	0.0332	0.0482	0.1376	0.5000
0.55	0.2283	4	0.9132					0.4500
0.60	0.1836	1	0.1836	1.3742	0.0229	0.0253	0.0722	0.4000
0.65	0.1434	4	0.5736					0.3500
0.70	0.1078	1	0.1078	0.8650	0.0144	0.0109	0.0311	0.3000
0.75	0.0700	4	0.2800					0.2500
0.80	0.0509	1	0.0509	0.4387	0.0073	0.0036	0.0103	0.2000
0.85	0.0299	4	0.1196					0.1500
0.90	0.0141	1	0.0141	0.1846	0.0031	0.0005	0.0014	0.1000
0.95	0.0039	4	0.0156					0.0499
1.00	0.0039	1	0.0000	0.0297	0.0005	0.0000	0.0000	0.0000
					(0.3504)			

Table C2: Numerical Solution of Equations 8, 9, and 10.
B = 0.2

x/L	f	Simpson's factor	Product	$y_0+4y_1+y_2$	da	$\frac{H_x}{H_f}$	H	Q_x/Q_0
0.00	1.0000	1	1.0000			(0.3128)	1.0000	1.0000
0.05	0.8489	4	3.3956					0.9153
0.10	0.7512	1	0.7512	5.1468	0.0858	0.2270	0.7257	0.8567
0.15	0.6657	4	2.6628					0.8025
0.20	0.5881	1	0.5881	4.0021	0.0667	0.1603	0.5125	0.7505
0.25	0.5169	4	2.0676					0.7000
0.30	0.4513	1	0.4513	3.1070	0.0518	0.1085	0.3469	0.6505
0.35	0.3907	4	1.5628					0.6017
0.40	0.3348	1	0.3348	2.3489	0.0391	0.0694	0.2219	0.5535
0.45	0.2834	4	1.1336					0.5058
0.50	0.2364	1	0.2364	1.7048	0.0284	0.0410	0.1311	0.4586
0.55	0.1936	4	0.7744					0.4117
0.60	0.1550	1	0.1550	1.1658	0.0194	0.0216	0.0691	0.3650
0.65	0.1206	4	0.4824					0.3188
0.70	0.0903	1	0.0903	0.7277	0.0121	0.0095	0.0304	0.2726
0.75	0.0643	4	0.2572					0.2268
0.80	0.0424	1	0.0424	0.3899	0.0065	0.0030	0.0096	0.1811
0.85	0.0248	4	0.0992					0.1356
0.90	0.0117	1	0.0117	0.1533	0.0026	0.0004	0.0013	0.0903
0.95	0.0032	4	0.0128					0.0451
1.00	0.0000	1	0.0000	0.0245	0.0004	0.0000	0.0000	0.0000
					(0.3128)			

Table C3: Numerical Solution of Equations 8, 9, and 10.

B = 0.4

x/L	f	Simpson's factor	Product	$y_0+4y_1+y_2$	da	$\frac{H_x}{H_f}$	H	Q_x/Q_0
0.00	1.0000	1	1.0000			(0.2770)	1.0000	1.0000
0.05	0.7903	4	3.1612					0.8806
0.10	0.6826	1	0.6826	4.8432	0.0807	0.1963	0.7087	0.8135
0.15	0.5947	4	2.3788					0.7551
0.20	0.5185	1	0.5185	3.5799	0.0597	0.1366	0.4931	0.7011
0.25	0.4507	4	1.8028					0.6500
0.30	0.3898	1	0.3898	2.7111	0.0452	0.0914	0.3300	0.6009
0.35	0.3346	4	1.3384					0.5534
0.40	0.2846	1	0.2846	2.0128	0.0335	0.0579	0.2090	0.5070
0.45	0.2393	4	0.9572					0.4617
0.50	0.1984	1	0.1984	1.4402	0.0240	0.0339	0.1224	0.4172
0.55	0.1616	4	0.6464					0.3734
0.60	0.1287	1	0.1287	0.9735	0.0162	0.0177	0.0639	0.3301
0.65	0.0997	4	0.3988					0.2875
0.70	0.0743	1	0.0743	0.6018	0.0100	0.0077	0.0278	0.2453
0.75	0.0526	4	0.2104					0.2036
0.80	0.0346	1	0.0346	0.3193	0.0053	0.0024	0.0087	0.1623
0.85	0.0202	4	0.0808					0.1212
0.90	0.0095	1	0.0095	0.1249	0.0021	0.0003	0.0011	0.0807
0.95	0.0026	4	0.0104					0.0401
1.00	0.0000	1	0.0000	0.0199	0.0003	0.0000	0.0000	0.0000
					(0.2770)			

Table C4: Numerical Solution of Equations 8, 9, and 10.
B = 0.6

x/L	f	Simpson's factor	Product	$y_0+4y_1+y_2$	da	$\frac{H_x}{H_f}$	H	Q_x/Q_0
0.00	1.0000	1	1.0000			(0.2439)	1.0000	1.0000
0.05	0.7336	4	2.9344					0.8458
0.10	0.6170	1	0.6170	4.5514	0.0759	0.1680	0.6888	0.7703
0.15	0.5274	4	2.1096					0.7076
0.20	0.4528	1	0.4528	3.1794	0.0530	0.1150	0.4715	0.6516
0.25	0.3887	4	1.5548					0.6000
0.30	0.3324	1	0.3324	2.3400	0.0390	0.0760	0.3116	0.5514
0.35	0.2826	4	1.1304					0.5050
0.40	0.2382	1	0.2382	1.7010	0.0284	0.0476	0.1952	0.4605
0.45	0.1987	4	0.7948					0.4175
0.50	0.1635	1	0.1635	1.1965	0.0199	0.0277	0.1136	0.3757
0.55	0.1323	4	0.5292					0.3350
0.60	0.1047	1	0.1047	0.7974	0.0133	0.0144	0.0590	0.2953
0.65	0.0806	4	0.3224					0.2563
0.70	0.0597	1	0.0597	0.4868	0.0081	0.0063	0.0258	0.2180
0.75	0.0421	4	0.1684					0.1804
0.80	0.0275	1	0.0275	0.2556	0.0043	0.0020	0.0005	0.1433
0.85	0.0160	4	0.0640					0.1068
0.90	0.0075	1	0.0075	0.0990	0.0017	0.0003	0.0012	0.0710
0.95	0.0020	4	0.0080					0.0352
1.00	0.0000	1	0.0000	0.0155	0.0003	0.0000	0.0000	0.0000
					(0.2439)			

Table C5: Numerical Solution of Equations 8, 9, and 10.
B = 0.8

x/L	f	Simpson's factor	Product	$y_0+4y_1+y_2$	da	$\frac{H_x}{H_f}$	H	Q_x/Q_0
0.00	1.0000	1	1.0000			(0.2127)	1.0000	1.0000
0.05	0.6789	4	2.7156					0.8111
0.10	0.5544	1	0.5544	4.2700	0.0712	0.1415	0.6654	0.7270
0.15	0.4638	4	1.8552					0.6602
0.20	0.3913	1	0.3913	2.8009	0.0467	0.0948	0.4458	0.6022
0.25	0.3309	4	1.3236					0.5500
0.30	0.2793	1	0.2793	1.9942	0.0332	0.0616	0.2897	0.5019
0.35	0.2346	4	0.9384					0.4567
0.40	0.1957	1	0.1957	1.4134	0.0236	0.0380	0.1787	0.4141
0.45	0.1616	4	0.6464					0.3733
0.50	0.1317	1	0.1317	0.9738	0.0162	0.0218	0.1025	0.3343
0.55	0.1056	4	0.4224					0.2967
0.60	0.0829	1	0.0829	0.6365	0.0106	0.0112	0.0527	0.2603
0.65	0.0633	4	0.2532					0.2250
0.70	0.0466	1	0.0466	0.3827	0.0064	0.0048	0.0226	0.1906
0.75	0.0326	4	0.1304					0.1572
0.80	0.0212	1	0.0212	0.1982	0.0033	0.0015	0.0071	0.1245
0.85	0.0122	4	0.0488					0.0924
0.90	0.0057	1	0.0057	0.0757	0.0013	0.0002	0.0009	0.0612
0.95	0.0015	4	0.0060					0.0303
1.00	0.0000	1	0.0000	0.0117	0.0002	0.0000	0.0000	0.0000
					(0.2127)			

Table C6: Numerical Solution of Equations 8, 9, and 10.
B = 1.0

x/L	f	Simpson's factor	Product	$y_0+4y_1+y_2$	da	$\frac{H_x}{H_f}$	H	Q_x/Q_0
0.00	1.0000	1	1.0000			(0.1840)	1.0000	1.0000
0.05	0.6261	4	2.5044					0.7764
0.10	0.4950	1	0.4950	3.9994	0.0667	0.1173	0.6375	0.6838
0.15	0.4040	4	1.6160					0.6127
0.20	0.3340	1	0.3340	2.4450	0.0408	0.0765	0.4158	0.5528
0.25	0.2774	4	1.1096					0.5000
0.30	0.2304	1	0.2304	1.6740	0.0279	0.0486	0.2641	0.4523
0.35	0.1908	4	0.7632					0.4084
0.40	0.1570	1	0.1570	1.1506	0.0192	0.0294	0.1598	0.3676
0.45	0.1280	4	0.5120					0.3292
0.50	0.1031	1	0.1031	0.7721	0.0129	0.0165	0.0897	0.2928
0.55	0.0818	4	0.3272					0.2584
0.60	0.0635	1	0.0635	0.4938	0.0082	0.0083	0.0451	0.2253
0.65	0.0480	4	0.1920					0.1938
0.70	0.0350	1	0.0350	0.2905	0.0048	0.0035	0.0190	0.1633
0.75	0.0243	4	0.0972					0.1340
0.80	0.0156	1	0.0156	0.1478	0.0025	0.0010	0.0054	0.1055
0.85	0.0089	4	0.0356					0.0780
0.90	0.0041	1	0.0041	0.0553	0.0009	0.0001	0.0005	0.0512
0.95	0.0011	4	0.0044					0.0253
1.00	0.0000	1	0.0000	0.0085	0.0001	0.0000	0.0000	0.0000
					(0.1840)			